Two flavor chiral phase transition from nonperturbative flow equations

J. Berges,* D.-U. Jungnickel,† and C. Wetterich‡
Institut für Theoretische Physik, Universität Heidelberg, Philosophenweg 16, 69120 Heidelberg, Germany
(Received 13 July 1998; published 8 January 1999)

We employ nonperturbative flow equations to compute the equation of state for two flavor QCD within an effective quark meson model. This yields the temperature and quark mass dependence of quantities such as the chiral condensate or the pion mass. A precision estimate of the universal critical equation of state for the three-dimensional $O(4)$ Heisenberg model is presented. We explicitly connect the $O(4)$ universal behavior near the critical temperature and zero quark mass with the physics at zero temperature and a realistic pion mass. For realistic quark masses the pion correlation length near T_c turns out to be smaller than its zero temperature value. [S0556-2821(98)06023-8]

PACS number(s): 12.39.Fe, 11.10.Hi, 11.10.Wx

I. INTRODUCTION

Strong interactions in thermal equilibrium at high temperature T—as realized in early stages of the evolution of the Universe—differ in important aspects from the well tested vacuum or zero temperature properties. A phase transition at some critical temperature T_c or a relatively sharp crossover may separate the high and low temperature physics [1]. Many experimental activities at heavy ion colliders [2] search for signs of such a transition. It was realized early that the transition should be closely related to a qualitative change in the chiral condensate according to the general observation that spontaneous symmetry breaking tends to be absent in a high temperature situation. A series of stimulating contributions [3–5] pointed out that for sufficiently small up and down quark masses, m_u and m_d, and for a sufficiently large mass of the strange quark, m_s, the chiral transition is expected to belong to the universality class of the $O(4)$ Heisenberg model. This means that near the critical temperature only the pions and the sigma particle play a role for the behavior of condensates and long distance correlation functions. It was suggested [4,5] that a large correlation length may be responsible for important fluctuations or lead to a disoriented chiral condensate [6]. This was even related [4,5] to the spectacular ''Centauro events'' [7] observed in cosmic rays. The question how small m_u and m_d would have to be in order to see a large correlation length near T_c and if this scenario could be realized for realistic values of the current quark masses remained, however, unanswered. The reason was the missing link between the universal behavior near T_c and zero current quark mass on one hand and the known physical properties at $T=0$ for realistic quark masses on the other hand.

It is the purpose of the present paper to provide this link. We present here the equation of state for two flavor QCD within an effective quark meson model. The equation of state expresses the chiral condensate $\langle\bar{\psi}\psi\rangle$ as a function of temperature and the average current quark mass $\hat{m}=(m_u+m_d)/2$. This connects explicitly the universal critical behavior for $T\to T_c$ and $\hat{m}\to 0$ with the temperature dependence for a realistic value $\hat{m}_{\rm phys}$. Since our discussion covers the whole temperature range $0\leqslant T\lesssim 1.7T_c$ we can fix $\hat{m}_{\rm phys}$ such that the (zero temperature) pion mass is $m_\pi=135$ MeV. The condensate $\langle\bar{\psi}\psi\rangle$ plays here the role of an order parameter. Its precise definition will be given in Sec. II. Figure 1 shows our results for $\langle\bar{\psi}\psi\rangle(T,\hat{m})$: Curve (a) gives the temperature dependence of $\langle\bar{\psi}\psi\rangle$ in the chiral limit $\hat{m}=0$. Here the lower curve is the full result for arbitrary T whereas the upper curve corresponds to the universal scaling form of the equation of state for the $O(4)$ Heisenberg model. We see perfect agreement of both curves for T sufficiently close to $T_c=100.7$ MeV. This demonstrates the capability of our method to cover the critical behavior and, in particular, to reproduce the critical exponents of the $O(4)$ model. We have determined (cf. Sec. V) the universal critical equation of state as well as the non-universal amplitudes. This provides the full functional dependence of $\langle\bar{\psi}\psi\rangle(T,\hat{m})$ for small $T-T_c$ and $\hat{m}$. The curves (b), (c) and (d) are for non-vanishing values of the average current quark mass $\hat{m}$. Curve (c) corresponds to $\hat{m}_{\rm phys}$ or, equivalently, $m_\pi(T=0)=135$ MeV. One observes a crossover in the range $T=(1.2-1.5)T_c$. The $O(4)$ universal equation of state (upper curve) gives a reasonable approximation in this temperature range. The transition turns out to be much less dramatic than for $\hat{m}=0$. We have also plotted in curve (b) the results for comparably small quark masses $\simeq 1$ MeV, i.e. $\hat{m}=\hat{m}_{\rm phys}/10$, for which the $T=0$ value of m_π equals 45 MeV. The crossover is considerably sharper but a substantial deviation from the chiral limit remains even for such small values of $\hat{m}$. In order to facilitate comparison with lattice simulations which are typically performed for larger values of m_π we also present results for $m_\pi(T=0)=230$ MeV in curve (d). One may define a ''pseudocritical temperature'' T_{pc} associated to the smooth crossover as the inflection point of $\langle\bar{\psi}\psi\rangle(T)$ as usually done in lattice simulations. Our results for this definition of T_{pc} are denoted by $T_{pc}^{(1)}$ and are presented in Table I for the four different values of $\hat{m}$ or,

*Current address: Center for Theoretical Physics, Massachusetts Institute of Technology, Cambridge, MA 02139.
Email address: Berges@ctp.mit.edu
†Email address: D.Jungnickel@thphys.uni-heidelberg.de
‡Email address: C.Wetterich@thphys.uni-heidelberg.de

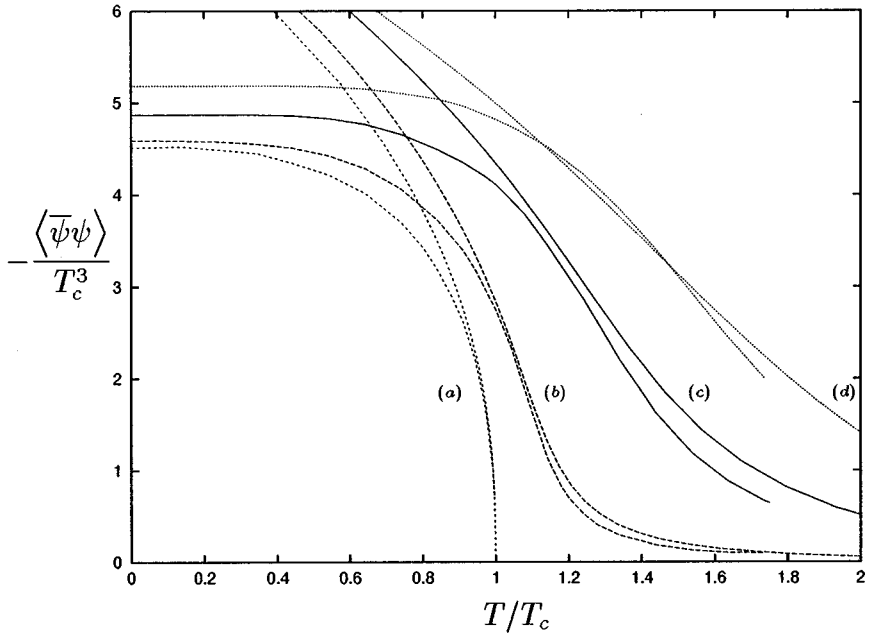

FIG. 1. The plot shows the chiral condensate $\langle\bar{\psi}\psi\rangle$ as a function of temperature T. Lines (a), (b), (c), (d) correspond at zero temperature to $m_\pi = 0$,45 MeV,135 MeV,230 MeV, respectively. For each pair of curves the lower one represents the full T dependence of $\langle\bar{\psi}\psi\rangle$ whereas the upper one shows for comparison the universal scaling form of the equation of state for the $O(4)$ Heisenberg model. The critical temperature for zero quark mass is $T_c = 100.7$ MeV. The chiral condensate is normalized at a scale $k_\Phi \simeq 620$ MeV.

equivalently, $m_\pi(T=0)$. The value for the pseudocritical temperature for $m_\pi = 230$ MeV compares well with the lattice results for two flavor QCD (cf. Sec. V). One should mention, though, that a determination of T_{pc} according to this definition is subject to sizeable numerical uncertainties for large pion masses as the curve in Fig. 1 is almost linear around the inflection point for quite a large temperature range. A problematic point in lattice simulations is the extrapolation to realistic values of m_π or even to the chiral limit. Our results may serve here as an analytic guide. The overall picture shows the approximate validity of the $O(4)$ scaling behavior over a large temperature interval in the vicinity of and above T_c once the (non-universal) amplitudes are properly computed.

A second important result of our investigations is the temperature dependence of the space-like pion correlation length $m_\pi^{-1}(T)$. [We will often call $m_\pi(T)$ the temperature dependent pion mass since it coincides with the physical pion mass for $T=0$.] The plot for $m_\pi(T)$ in Fig. 2 again shows the second order phase transition in the chiral limit $\hat{m}=0$. For $T<T_c$ the pions are massless Goldstone bosons whereas for $T>T_c$ they form with the sigma particle a degenerate vector of $O(4)$ with mass increasing as a function of temperature. For $\hat{m}=0$ the behavior for small positive $T-T_c$ is characterized by the critical exponent ν, i.e. $m_\pi(T) = (\xi^+)^{-1} T_c((T-T_c)/T_c)^\nu$ and we obtain $\nu = 0.787$, $\xi^+ = 0.270$. For $\hat{m}>0$ we find that $m_\pi(T)$ remains almost constant for $T \lesssim T_c$ with only a very slight dip for T near $T_c/2$. For $T>T_c$ the correlation length decreases rapidly and for $T \gg T_c$ the precise value of $\hat{m}$ becomes irrelevant. We see that the universal critical behavior near T_c is quite smoothly connected to $T=0$. The full functional dependence of $m_\pi(T,\hat{m})$ allows us to compute the overall size of the pion correlation length near the critical temperature and we find $m_\pi(T_{pc}) \simeq 1.7 m_\pi(0)$ for the realistic value $\hat{m}_{\rm phys}$. This correlation length is even smaller than the vacuum $(T=0)$ one and gives no indication for strong fluctuations of pions with long wavelength. It would be interesting to see if a decrease of the pion correlation length at and above T_c is experimentally observable. It should be emphasized, however, that a tricritical behavior with a massless excitation remains possible for three flavors. This would not be characterized by the universal behavior of the $O(4)$ model. We also point out that the present investigation for the two flavor case does not take into account a speculative ''effective restoration'' of the axial $U_A(1)$ symmetry at high temperature [3,8]. We will comment on these issues in Sec. VI.

TABLE I. The table shows the critical and ''pseudocritical'' temperatures for various values of the zero temperature pion mass. Here $T_{pc}^{(1)}$ is defined as the inflection point of $\langle\bar{\psi}\psi\rangle(T)$ whereas $T_{pc}^{(2)}$ is the location of the maximum of the sigma correlation length (see Sec. IV).

$\frac{m_\pi}{\rm MeV}$	0	45	135	230
$\frac{T_{pc}^{(1)}}{\rm MeV}$	100.7	$\simeq 110$	$\simeq 130$	$\simeq 150$
$\frac{T_{pc}^{(2)}}{\rm MeV}$	100.7	113	128	—

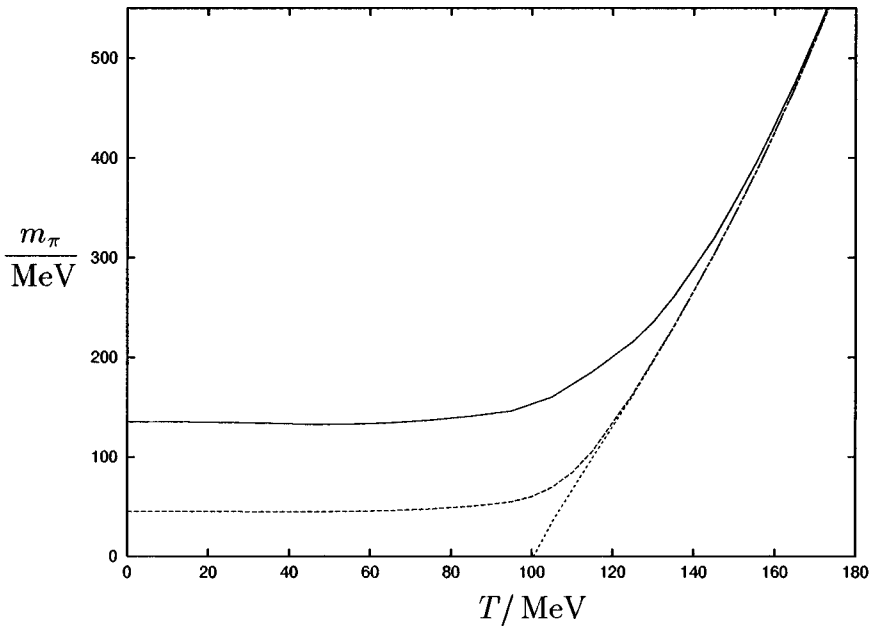

FIG. 2. The plot shows m_π as a function of temperature T for three different values of the average light current quark mass $\hat{m}$. The solid line corresponds to the realistic value $\hat{m}=\hat{m}_{\mathrm{phys}}$ whereas the dotted line represents the situation without explicit chiral symmetry breaking, i.e., $\hat{m}=0$. The intermediate, dashed line assumes $\hat{m}=\hat{m}_{\mathrm{phys}}/10$.

Our method is based on the effective average action Γ_k [9] which is the generating functional of the $1PI$ Green functions in presence of an infrared cutoff k. In a thermal equilibrium context Γ_k depends also on temperature and describes a coarse grained free energy as a functional of appropriate fields. Here k^{-1} corresponds to the coarse graining length scale. Varying the infrared cutoff k allows us to consider the relevant physics in dependence on some momentum-like scale. The results for the order parameter and correlation functions presented in this paper are obtained by removing the infrared cutoff $(k\to 0)$ in the end. For scalar fields Φ_i the k dependence of the effective average action is given by an exact nonperturbative flow equation [10]

$$\frac{\partial}{\partial t}\Gamma_k[\Phi]=\frac{1}{2}\,\mathrm{Tr}\left\{(\Gamma_k^{(2)}[\Phi]+R_k)^{-1}\frac{\partial R_k}{\partial t}\right\} \tag{1.1}$$

where $t=\ln(k/\Lambda)$ with Λ an arbitrary momentum scale. Here $\Gamma_k^{(2)}$ denotes the matrix of second functional derivatives of Γ_k with respect to the field components:

$$(\Gamma_k^{(2)})_{ij}[\Phi](q,q')=\frac{\delta^2\Gamma_k[\Phi]}{\delta\Phi^i(q)\,\delta\Phi^j(-q')} \tag{1.2}$$

and we employ a momentum dependent infrared cutoff

$$R_k(q)=\frac{Z_{\Phi,k}q^2e^{-q^2/k^2}}{1-e^{-q^2/k^2}} \tag{1.3}$$

with $Z_{\Phi,k}$ an appropriate wave function renormalization constant to be specified later. In momentum space the trace contains a momentum integration, $\mathrm{Tr}=\int[d^dq/(2\pi)^d]\Sigma_i$. The flow equation (1.1) closely resembles a one-loop equation: Indeed, replacing $\Gamma_k^{(2)}$ by the second functional derivative of the classical action, $S_{\mathrm{cl}}^{(2)}$, it corresponds to the one-loop result for a theory where an infrared cutoff

$$\frac{1}{2}\int\frac{d^dq}{(2\pi)^d}\,\varphi_i(q)R_k(q)\varphi_i(-q)$$

is added to the classical action $S_{\mathrm{cl}}[\varphi]$. This cutoff appears in the inverse ''average propagator''

$$P(q)=q^2+Z_{\Phi,k}^{-1}R_k(q)=\frac{q^2}{1-\exp\left\{-\dfrac{q^2}{k^2}\right\}} \tag{1.4}$$

which approaches k^2 for $q^2\ll k^2$. Up to exponentially small corrections the integration of the high momentum modes with $q^2\gg k^2$ is not affected by the infrared cutoff. The ''renormalization group improvement'' $S_{\mathrm{cl}}^{(2)}\to\Gamma_k^{(2)}$ contains all contributions beyond one-loop and makes Eq. (1.1) exact. Of course, it also turns the flow equation into a functional differential equation which cannot be solved exactly in general. We emphasize that the flow equation (1.1) is connected to the Wilsonian renormalization group equation [11–15] (often also called exact renormalization group equation). Extensions of the flow equations to fermions [16,17] and gauge fields [18–24] are available.

Since in most cases the flow equation can not be solved exactly the capacity to devise useful truncations in a nonperturbative context becomes crucial. This requires first of all an identification of the degrees of freedom which are most relevant for a given problem. In the present paper we concentrate on the chiral aspects of QCD.[1] Spontaneous chiral symmetry breaking occurs through the expectation value of a (complex) scalar field Φ_{ab} which transforms as $(\bar{\mathbf{N}},\mathbf{N})$ under

[1]For a study of chiral symmetry breaking in QED using related exact renormalization group techniques see Ref. [25].

the chiral flavor group $SU_L(N)\times SU_R(N)$ with N the number of light quark flavors. More precisely, the expectation value

$$\langle \Phi^{ab}\rangle = \bar{\sigma}_0 \delta^{ab} \tag{1.5}$$

induces for $\bar{\sigma}_0 \neq 0$ a spontaneous breaking of the chiral group to a vector-like subgroup, $SU_L(N)\times SU_R(N) \to SU_{L+R}(N) \equiv SU_V(N)$. In addition, non-vanishing current quark masses m_u, m_d, m_s break the chiral group explicitly and also lift the $SU_V(N)$ degeneracy of the spectrum if they are unequal. The physical degrees of freedom contained in the field Φ_{ab} are pseudoscalar and scalar mesons which can be understood as quark-antiquark bound states. It is obvious that any analytical description of the chiral transition has to include at least part of these (pseudo)scalar fields as the most relevant degrees of freedom.

In the present work we use for k smaller than a ''compositeness scale'' $k_\Phi \simeq 600$ MeV a description in terms of Φ_{ab} and quark degrees of freedom. The quarks acquire a constituent quark mass M_q through the chiral condensate $\bar{\sigma}_0$ which forms in our picture for $k_{\chi SB} \simeq 400$ MeV. This effective quark meson model can be obtained from QCD by ''integrating out'' the gluon degrees of freedom and introducing fields for composite operators [26,22]. This will be explained in more detail in the first part of Sec. II. In this picture the scale k_Φ is associated to the scale at which the formation of mesonic bound states can be observed in the flow of the effective (momentum dependent) four-quark interaction. We will restrict our discussion in this paper to two flavor QCD with equal quark masses $m_u = m_d \equiv \hat{m}$. Since in this case the scalar triplet a_0 and the pseudoscalar singlet (associated with the η') have typical masses around[2] 1 GeV we will neglect them for $k < k_\Phi$. This reduces the scalar degrees of freedom of our effective model to a four component vector of $O(4)$, consisting of the three pions and the ''sigma resonance.''

We imagine that all other degrees of freedom besides the quarks ψ and the scalars Φ are integrated out. This is reflected in the precise form of the effective average action $\Gamma_{k_\Phi}[\psi,\Phi]$ at the scale k_Φ which serves as an initial value for the solution of the flow equation. The flow of $\Gamma_k[\psi,\Phi]$ for $k < k_\Phi$ is then entirely due to the quark and meson fluctuations which are not yet included in $\Gamma_{k_\Phi}[\psi,\Phi]$. Obviously, the initial value Γ_{k_Φ} may be a quite complicated functional of ψ and Φ containing, in particular, important non-local behavior. We will nevertheless use a rather simple truncation in terms of standard kinetic terms and a most general form of the scalar potential U_k, i.e.[3]

$$\hat{\Gamma}_k = \Gamma_k - \frac{1}{2}\int d^4x \ \mathrm{tr}(\Phi^\dagger J + J^\dagger \Phi)$$

$$\Gamma_k = \int d^4x \Big\{ Z_{\psi,k}\bar{\psi}_a i\not{\partial}\psi^a + Z_{\Phi,k}\ \mathrm{tr}[\partial_\mu \Phi^\dagger \partial^\mu \Phi] + U_k(\Phi,\Phi^\dagger) + \bar{h}_k \bar{\psi}^a \Big(\frac{1+\gamma_5}{2}\Phi_{ab} - \frac{1-\gamma_5}{2}(\Phi^\dagger)_{ab}\Big)\psi^b \Big\}. \tag{1.6}$$

Here Γ_k is invariant under the chiral flavor symmetry $SU_L(2)\times SU_R(2)$ and the only explicit symmetry breaking arises through the source term $J \sim \hat{m}$. We will consider the flow of the most general form of U_k consistent with the symmetries (without any restriction to a polynomial form as typically used in a perturbative context). On the other hand, our approximations for the kinetic terms are rather crude and parameterized by only two running wave function renormalization constants, $Z_{\Phi,k}$ and $Z_{\psi,k}$. The same holds for the effective Yukawa coupling $\bar{h}_k$. The main approximations in this work concern

(i) the simple form of the derivative terms and the Yukawa coupling, in particular, the neglect of higher derivative terms (and terms with two derivatives and higher powers of Φ). This is partly motivated by the observation that at the scale k_Φ and for small temperatures the possible strong non-localities related to confinement affect most likely only the quarks in a momentum range $q^2 \lesssim (300\ \mathrm{MeV})^2$. Details of the quark propagator and interactions in this momentum range are not very important in our context (see Sec. II).

(ii) the neglect of interactions involving more than two quark fields. This is motivated by the fact that the dominant multi-quark interactions are already incorporated in the mesonic description. Six-quark interactions beyond those contained effectively in U_k could be related to baryons and play probably only a minor role for the meson physics considered here.

We will choose a normalization of ψ,Φ such that $Z_{\psi,k_\Phi} = \bar{h}_{k_\Phi} = 1$. We therefore need as initial values at the scale k_Φ the scalar wave function renormalization Z_{Φ,k_Φ} and the shape of the potential U_{k_Φ}. We will make here the important assumption that $Z_{\Phi,k}$ is small at the compositeness scale k_Φ (similarly to what is usually assumed in Nambu–Jona-Lasinio-like models). This results in a large value of the renormalized Yukawa coupling $h_k = Z_{\Phi,k}^{-1/2} Z_{\psi,k}^{-1} \bar{h}_k$. A large value of h_{k_Φ} is phenomenologically suggested by the comparably large value of the constituent quark mass M_q. The latter is related to the value of the Yukawa coupling for $k \to 0$ and the pion decay constant $f_\pi = 92.4$ MeV by $M_q = h f_\pi/2$ (with $h = h_{k=0}$), and $M_q \simeq 300$ MeV implies $h^2/4\pi \simeq 3.4$. For increasing k the value of the Yukawa coupling grows rapidly for $k \gtrsim M_q$. Our assumption of a large

[2]More precisely, because of the anomalous $U_A(1)$ breaking in QCD these mesons are significantly heavier than the remaining degrees of freedom in the range of scales k where the dynamics of the model is strongly influenced by mesonic fluctuations. The situation becomes more involved if the model is considered at high temperature which is discussed in Sec. VI.

[3]Our Euclidean conventions ($\bar{h}_k$ is real) are specified in Refs. [27, 16].

initial value for h_{k_Φ} is therefore equivalent to the assumption that the truncation (1.6) can be used up to the vicinity of the Landau pole of h_k. The existence of a strong Yukawa coupling enhances the predictive power of our approach considerably. It implies a fast approach of the running couplings to partial infrared fixed points [27]. In consequence, the detailed form of U_{k_Φ} becomes unimportant, except for the value of one relevant parameter corresponding to the scalar mass term $\bar{m}^2_{k_\Phi}$. In this paper we fix $\bar{m}^2_{k_\Phi}$ such that $f_\pi = 92.4$ MeV for $m_\pi = 135$ MeV. The possibility of such a choice is highly non-trivial since f_π can actually be predicted [27] in our setting within a relatively narrow range. The value $f_\pi = 92.4$ MeV (for $m_\pi = 135$ MeV) sets our unit of mass for two flavor QCD which is, of course, not directly accessible by observation. In addition to $\bar{m}^2_{k_\Phi}$ (or f_π) the other input parameter used in this work is the constituent quark mass M_q which determines the scale k_Φ at which h_{k_Φ} becomes very large. We consider a range 300 MeV$\lesssim M_q \lesssim$350 MeV and find a rather weak dependence of our results on the precise value of M_q. We also observe that the limit $h_{k_\Phi} \to \infty$ can be considered as the lowest order of a systematic expansion in $h^{-1}_{k_\Phi}$ which is obviously highly nonperturbative.

A generalization of our method to the realistic case of three light flavors is possible and work in this direction is in progress. For the time being we expect that many features found for $N=2$ will carry over to the realistic case, especially the critical behavior for $T \to T_c$ and $\hat{m} \to 0$ (for fixed $m_s \neq 0$). Nevertheless, some quantities like $\langle \bar{\psi}\psi \rangle (T=0)$, the difference between f_π for realistic quark masses and $\hat{m}=0$ or the mass of the sigma resonance at $T=0$ may be modified. This will also affect the non-universal amplitudes in the critical equation of state and, in particular, the value of T_c. In the picture of the two flavor quark meson model these changes occur through an effective temperature dependence of the initial values of couplings at the scale k_Φ. This effect, which is due to the temperature dependence of effects from fluctuations not considered in the present work is discussed briefly in Sec. VI. It remains perfectly conceivable that this additional temperature dependence may result in a first order phase transition or a tricritical behavior for realistic values of $\hat{m}$ for the three flavor case. Details will depend on the strange quark mass. We observe, however, that the temperature dependence in the limit $\hat{m} \to 0$ involves for $T \lesssim T_c$ only information from the running of couplings in the range $k \lesssim 300$ MeV. (The running for $k \gtrsim 3T$ effectively drops out in the comparison between the thermal equilibrium results and those for $T=0$.) In this range of temperatures our model should be quite reliable.

Finally, we mention that we have concentrated here only on the Φ-dependent part of the effective action which is related to chiral symmetry breaking. The Φ-independent part of the free energy also depends on T and only part of this temperature dependence is induced by the scalar and quark fluctuations considered in the present paper. Most likely, the gluon degrees of freedom cannot be neglected for this purpose. This is the reason why we do not give results for ''overall quantities'' like energy density or pressure as a function of T.

This paper is organized as follows: In Sec. II we review the linear quark meson model at vanishing temperature. We begin with an overview of the different scales appearing in strong interaction physics. Subsequently, the flow equations for the linear quark meson model are introduced and their approximate partial fixed point behavior is discussed in detail leading to a ''prediction'' of the chiral condensate $\langle \bar{\psi}\psi \rangle$. In Sec. III the exact renormalization group formulation of field theories in thermal equilibrium is given. It is demonstrated how mass threshold functions in the flow equations smoothly decouple all massive Matsubara modes as the temperature increases, therefore leading to a ''dimensional reduction'' of the model. Section IV contains our results for the linear quark meson model at non-vanishing temperature. Here we discuss the T dependences of the parameters and physical observables of the linear quark meson model in detail for a temperature range $0 \leqslant T \lesssim 170$ MeV including the (pseudo)critical temperature T_c of the chiral transition. The critical behavior of the model near T_c and $\hat{m}=0$, where $\hat{m}$ denotes the light average current quark mass, is carefully analyzed in Sec. V. There we present the universal scaling form of the equation of state including a fit for the corresponding scaling function. Also the universal critical exponents and amplitude ratios are given there. The effects of additional degrees of freedom of strong interaction physics not included in the linear $O(4)$-symmetric quark meson model are addressed in Sec. VI. Here we also comment on differences between the linear quark meson model and chiral perturbation theory. Some technical details concerning the quark mass term and the definition of threshold functions at vanishing and non-vanishing temperature are presented in three appendices.

II. THE QUARK MESON MODEL AT $T=0$

Before discussing the finite temperature behavior of strong interaction physics we will review some of its zero temperature features. This will be done within the framework of a linear quark meson model as an effective description for QCD for scales below the mesonic compositeness scale of approximately $k_\Phi \simeq 600$ MeV. Relating this model to QCD in a semi-quantitative way in Sec. II A will allow us to gain some information on the initial value for the effective average action at the compositeness scale k_Φ. We emphasize, however, that the quantitative aspects of the derivation of the effective quark meson model from QCD will not be relevant for our practical calculations in the mesonic sector. This is related to the ''infrared stability'' for large Yukawa coupling h_{k_Φ} as discussed in the Introduction and which will be made quantitative in Sec. II B.

A. A short (scale) history of QCD

For an evaluation of the trace on the right hand side of the flow equation (1.1) only a small momentum range $q^2 \simeq k^2$ contributes substantially. One therefore only needs to take

into account those fluctuations which are important in this momentum interval. Here we are interested in the description of chiral symmetry breaking. The relevant fluctuations in relation to this phenomenon may change with the scale k and we begin by summarizing the qualitatively different scale intervals which appear for meson physics in QCD. Some of this will be explained in more detail in the remainder of this section whereas other aspects are well known. Details of this discussion may also be found in Refs. [26–28]. We will distinguish five qualitatively different ranges of scales:

(1) At sufficiently high momentum scales, say,
$$k \gtrsim k_p \simeq 1.5 \text{ GeV}$$
the relevant degrees of freedom of strong interactions are quarks and gluons and their dynamics is well described by perturbative QCD.

(2) For decreasing momentum scales in the range
$$k_\Phi \simeq 600 \text{ MeV} \lesssim k \lesssim k_p \simeq 1.5 \text{ GeV}$$
the dynamical degrees of freedom are still quarks and gluons. Yet, as k is lowered part of their dynamics becomes dominated by effective non-local four quark interactions which cannot be fully accessed perturbatively.

(3) At still lower scales this situation changes dramatically. Quarks and gluons are supplemented by mesonic bound states as additional degrees of freedom which are formed at a scale $k_\Phi \simeq 600$ MeV. We emphasize that k_Φ is well separated from $\Lambda_{\rm QCD} \simeq 200$ MeV where confinement sets in and from the constituent masses of the quarks $M_q \simeq (300-350)$ MeV. This implies that below the compositeness scale k_Φ there exists a hybrid description in term of quarks *and* mesons. It is important to note that for scales not too much smaller than k_Φ chiral symmetry remains unbroken. This situation holds down to a scale $k_{\chi SB} \simeq 400$ MeV at which the scalar meson potential develops a non-trivial minimum thus breaking chiral symmetry spontaneously. The meson dynamics within the range
$$k_{\chi SB} \simeq 400 \text{ MeV} \lesssim k \lesssim k_\Phi \simeq 600 \text{ MeV}$$
is dominated by light current quarks with a strong Yukawa coupling $h_k^2/(4\pi) \gg \alpha_s(k)$ to mesons. We will thus assume that the leading gluon effects are included below k_Φ already in the formation of mesons. Near $k_{\chi SB}$ also fluctuations of the light scalar mesons become important as their initially large renormalized mass approaches zero. Other hadronic bound states like vector mesons or baryons should have masses larger than those of the lightest scalar mesons, in particular near $k_{\chi SB}$, and give therefore only subleading contributions to the dynamics. This leads us to a simple linear model of quarks and scalar mesons as an effective description of QCD for scales below k_Φ.

(4) As one evolves to scales below $k_{\chi SB}$ the Yukawa coupling decreases whereas α_s increases. Of course, getting closer to $\Lambda_{\rm QCD}$ it is no longer justified to neglect in the quark sector the QCD effects which go beyond the dynamics of the effective quark meson model in our truncation (1.6). On the other hand, the final IR value of the Yukawa coupling h is fixed by the typical values of constituent quark masses $M_q \simeq 300$ MeV to be $h^2/(4\pi) \simeq 3.4$. One may therefore speculate that the domination of the Yukawa interaction persists even for the interval
$$M_q \simeq 300 \text{ MeV} \lesssim k \lesssim k_{\chi \rm SB} \simeq 400 \text{ MeV}$$
below which the quarks decouple from the evolution of the mesonic degrees of freedom altogether. Of course, details of the gluonic interactions are expected to be crucial for an understanding of quark and gluon confinement. Strong interaction effects may dramatically change the momentum dependence of the quark propagator for k and q^2 around $\Lambda_{\rm QCD}$. Yet, there is no coupling of the gluons to the color neutral mesons. As long as one is only interested in the dynamics of the mesons one is led to expect that confinement effects are quantitatively not too important.

(5) Because of the effective decoupling of the quarks and therefore of the whole colored sector the details of confinement have only little influence on the mesonic dynamics for scales
$$k \lesssim M_q \simeq 300 \text{ MeV}.$$
Here quarks and gluons disappear effectively from the spectrum and one is left with the pions. They are the only particles whose propagation is not suppressed by a large mass. For scales below the pion mass the flow of the couplings stops.

Let us now try to understand these different ranges of scales in more detail. We may start at $k_p = 1.5$ GeV where we assume that all gluonic degrees of freedom have been integrated out while we have kept an effective infrared cutoff $\sim k_p$ in the quark propagators. Details of this procedure were outlined in Ref. [22]. This results in a non-trivial momentum dependence of the quark propagator and effective non-local four and higher quark interactions. Because of the infrared cutoff the resulting effective action for the quarks resembles closely the one for heavy quarks (at least for Euclidean momenta). The dominant effect is the appearance of an effective quark potential similar to the one for the charm quark which describes the effective four quark interactions.

We next have to remove the infrared cutoff for the quarks, $k \to 0$. This task can be carried out by means of the exact flow equation for quarks only, starting at k_p with an initial value $\Gamma_{k_p}[\psi]$ as obtained after integrating out the gluons. A first investigation in this direction [26] used a truncation with a chirally invariant four quark interaction whose most general momentum dependence was retained. A crucial point is, of course, the initial value for this momentum dependence at k_p. The ansatz used in Ref. [26] is obtained by Fierz transforming the heavy quark potential and keeping, for simplicity, only the scalar meson channel while neglecting the ρ-meson and pomeron channels which are also present. The effective heavy quark potential was approximated there by a one gluon exchange term $\sim \alpha_s(k_p)$ supplemented by a linearly rising string tension term. This ansatz corresponds to the four quark interaction generated by the flavor neutral t-channel one gluon exchange depicted in Fig. 3 with an

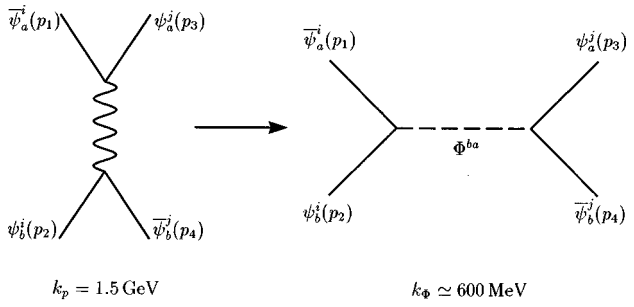

FIG. 3. The left diagram represents the one gluon exchange t-channel contribution to the four quark vertex at the scale $k_p \simeq 1.5$ GeV. It is assumed here that the gluon propagator is modified such that it accounts for the linearly rising term in the heavy quark potential. The right diagram displays the scalar meson s-channel exchange found at the compositeness scale $k_\Phi \simeq 600$ MeV.

appropriately modified gluon propagator and quark gluon vertex in order to account for the linearly rising part of the potential.

The evolution equation for the four quark interaction can be derived from the fermionic version of Eq. (1.1). It is by far not clear that the evolution of the effective four quark vertex will lead at lower scales to a momentum dependence representing the (s-channel) exchange of colorless mesonic bound states. Yet, at the compositeness scale

$$k_\Phi \simeq 600\ \mathrm{MeV} \tag{2.1}$$

one finds [26] an approximate Bethe-Salpeter factorization of the four quark amplitude with precisely this property. This situation is described by the right Feynman diagram in Fig. 3. In particular, it was possible to extract the amputated Bethe-Salpeter wave function as well as the mesonic bound state propagator displaying a pole-like structure in the s channel if it is continued to negative $s=(p_1+p_2)^2$. In the limit where the momentum dependence of the Bethe-Salpeter wave function and the bound state propagator is neglected the effective action Γ_{k_Φ} resembles[4] the Nambu–Jona-Lasinio model [29,30]. It is therefore not surprising that our description of the dynamics for $k<k_\Phi$ will parallel certain aspects of the investigations of this model, even though we are not bound to the approximations used typically in such studies (large-N_c expansion, perturbative renormalization group, etc.).

It is clear that for scales $k \lesssim k_\Phi$ a description of strong interaction physics in terms of quark fields alone would be rather inefficient. Finding physically reasonable truncations of the effective average action should be much easier once composite fields for the mesons are introduced. The exact renormalization group equation can indeed be supplemented by an exact formalism for the introduction of composite field variables or, more generally, a change of variables [26]. In the context of QCD this amounts to the replacement of the dominant part of the four quark interactions by scalar meson fields with Yukawa couplings to the quarks. In turn, this substitutes the effective quark action at the scale k_Φ by the effective quark meson action given in Eq. (1.6) in the Introduction.[5] The term in the effective potential U_{k_Φ} which is quadratic in Φ, $U_{k_\Phi}=\bar{m}^2_{k_\Phi}\ \mathrm{tr}\ \Phi^\dagger\Phi+\cdots$, turns out to be positive as a consequence of the attractiveness of the four quark interaction inducing it. Its value was found for the simple truncations used in Ref. [26] to be $\bar{m}_{k_\Phi}\simeq 120$ MeV. The higher order terms in U_{k_Φ} cannot be determined in the four quark approximation since they correspond to terms involving six or more quark fields. (Their values will not be needed for our quantitative investigations as is discussed in Sec. II B.) The initial value of the (bare) Yukawa coupling corresponds to the amputated Bethe-Salpeter wave function. Neglecting its momentum dependence it can be normalized to $\bar{h}_{k_\Phi}=1$. Moreover, the quark wave function renormalization $Z_{\psi,k}$ is normalized to one at the scale k_Φ for convenience. One may add that we have refrained here for simplicity from considering four quark operators with vector and pseudo-vector spin structure. Their inclusion is straightforward and would lead to vector and pseudo-vector mesons in the effective action.

In view of the possible large truncation errors made in Ref. [26] we will take Eq. (2.1) and the above value of $\bar{m}_{k_\Phi}$ only as order of magnitude estimates. Furthermore, we will assume, as motivated in the Introduction and usually done in large-N_c computations within the NJL model, that

$$Z_{\Phi,k_\Phi} \ll 1. \tag{2.2}$$

As a consequence, the initial value of the renormalized Yukawa coupling $h_{k_\Phi}=Z^{-1/2}_{\Phi,k_\Phi}Z^{-1}_{\psi,k_\Phi}\bar{h}_{k_\Phi}$ is much larger than one and we will be able to exploit the infrared stable features of the flow equations. As a typical coupling we take $h_{k_\Phi}=100$ in order to simulate the limit $h_{k_\Phi}\to\infty$. The effective potential $U_k(\Phi)$ must be invariant under the chiral $SU_L(N)\times SU_R(N)$ flavor symmetry. In fact, the axial anomaly of QCD breaks the Abelian $U_A(1)$ symmetry. The resulting $U_A(1)$ violating multi-quark interactions[6] lead to corresponding $U_A(1)$ violating terms in $U_k(\Phi)$. Accordingly, the most general effective potential U_k is a function of the $N+1$ independent C and P conserving $SU_L(N)\times SU_R(N)$ invariants

$$\rho=\mathrm{tr}\ \Phi^\dagger\Phi,$$

[4]Our solution of the flow equation for Γ_k with $Z_{\Phi,k_\Phi}=0$ (see below) may be considered as a solution of the NJL model with a particular form of the ultraviolet cutoff dictated by the shape of $R_k(q^2)$ as given in Eq. (1.3).

[5]We note that no double counting problem arises in this procedure.

[6]A first attempt for the computation of the anomaly term in the fermionic effective average action can be found in Ref. [31].

$$\tau_i \sim \mathrm{tr}\left(\Phi^\dagger\Phi - \frac{1}{N}\rho\right)^i, \quad i=2,\ldots,N,$$

$$\xi = \det\Phi + \det\Phi^\dagger. \tag{2.3}$$

For a given initial form of U_k all quantities in our truncation of Γ_k (1.6) are now fixed and we may follow the flow of Γ_k to $k\to 0$. In this context it is important that the formalism for composite fields [26] also induces an infrared cutoff in the meson propagator. The flow equations are therefore exactly of the form (1.1), with quarks and mesons treated on an equal footing. At the compositeness scale the quadratic term of $U_{k_\Phi} = \bar{m}^2_{k_\Phi}\,\mathrm{Tr}\,\Phi^\dagger\Phi + \cdots$ is positive and the minimum of U_{k_Φ} therefore occurs for $\Phi = 0$. Spontaneous chiral symmetry breaking is described by a non-vanishing expectation value $\langle\Phi\rangle$ in absence of quark masses. This follows from the change of the shape of the effective potential U_k as k flows from k_Φ to zero. The large renormalized Yukawa coupling rapidly drives the scalar mass term to negative values and leads to a potential minimum away from the origin at some scale $k_{\chi\mathrm{SB}} < k_\Phi$ such that finally $\langle\Phi\rangle = \bar{\sigma}_0 \neq 0$ for $k\to 0$ [26,27]. This concludes our overview of the general features of chiral symmetry breaking in the context of flow equations for QCD.

We will concentrate in this work on the two flavor case ($N=2$) and comment on the effects of including the strange quark in section 6. Furthermore we will neglect isospin violation and therefore consider a singlet source term J proportional to the average light current quark mass $\hat{m} \equiv \frac{1}{2}(m_u + m_d)$. Due to the $U_A(1)$ anomaly there is a mass split for the mesons described by Φ. The scalar triplet (a_0) and the pseudoscalar singlet (η') receive a large mass whereas the pseudoscalar triplet (π) and the scalar singlet (σ) remains light. From the measured values $m_{\eta'}, m_{a_0} \simeq 1$ GeV it is evident that a decoupling of these mesons is presumably a very realistic limit.[7] It can be achieved in a chirally invariant way and leads to the well known $O(4)$-symmetric Gell-Mann–Levy linear sigma model [32] which is, however, coupled to quarks now. This is the two flavor linear quark meson model which we will study in the remainder of this work. For this model the effective potential U_k is a function of ρ only.

It remains to determine the source J as a function of the average current quark mass $\hat{m}$. This is carried out in Appendix A and we obtain in our normalization with $Z_{\psi,k_\Phi} = 1$, $\bar{h}_{k_\Phi} = 1$,

$$J = 2\bar{m}^2_{k_\Phi}\hat{m}. \tag{2.4}$$

It is remarkable that higher order terms do not influence the relation between J and $\hat{m}$. Only the quadratic term $\bar{m}^2_{k_\Phi}$ enters which is in our scenario the only relevant coupling. This feature is an important ingredient for the predictive power of the model as far as the absolute size of the current quark mass is concerned.

The quantities which are directly connected to chiral symmetry breaking depend on the k-dependent expectation value $\langle\Phi\rangle_k = \bar{\sigma}_{0,k}$ as given by

$$\frac{\partial U_k}{\partial\rho}(\rho = 2\bar{\sigma}^2_{0,k}) = \frac{J}{2\bar{\sigma}_{0,k}}. \tag{2.5}$$

In terms of the renormalized expectation value

$$\sigma_{0,k} = Z^{1/2}_{\Phi,k}\bar{\sigma}_{0,k} \tag{2.6}$$

we obtain the following expressions for phenomenological observables from Eq. (1.6) for[8] $d=4$

$$f_{\pi,k} = 2\sigma_{0,k},$$

$$\langle\bar{\psi}\psi\rangle_k = -2\bar{m}^2_{k_\Phi}[Z^{-1/2}_{\Phi,k}\sigma_{0,k} - \hat{m}],$$

$$M_{q,k} = h_k\sigma_{0,k},$$

$$m^2_{\pi,k} = Z^{-1/2}_{\Phi,k}\frac{\bar{m}^2_{k_\Phi}\hat{m}}{\sigma_{0,k}} = Z^{-1/2}_{\Phi,k}\frac{J}{2\sigma_{0,k}},$$

$$m^2_{\sigma,k} = Z^{-1/2}_{\Phi,k}\frac{\bar{m}^2_{k_\Phi}\hat{m}}{\sigma_{0,k}} + 4\lambda_k\sigma^2_{0,k}. \tag{2.7}$$

Here we have defined the dimensionless, renormalized couplings

$$\lambda_k = Z^{-2}_{\Phi,k}\frac{\partial^2 U_k}{\partial\rho^2}(\rho = 2\bar{\sigma}^2_{0,k}),$$

$$h_k = Z^{-1/2}_{\Phi,k}Z^{-1}_{\psi,k}\bar{h}_k. \tag{2.8}$$

We will mainly be interested in the ''physical values'' of the quantities (2.7) in the limit $k\to 0$ where the infrared cutoff is removed, i.e. $f_\pi = f_{\pi,k=0}$, $m^2_\pi = m^2_{\pi,k=0}$, etc. We point out that the formalism of composite fields provides the link [26] to the chiral condensate $\langle\bar{\psi}\psi\rangle$ since the expectation value $\bar{\sigma}_0$ is related to the expectation value of a composite quark-antiquark operator.

B. Flow equations and infrared stability

At first sight, a reliable computation of $\Gamma_{k\to 0}$ seems a very difficult task. Without a truncation Γ_k is described by an infinite number of parameters (couplings, wave function renormalizations, etc.) as can be seen if Γ_k is expanded in powers of fields and derivatives. For instance, the sigma mass is obtained as a zero of the exact inverse propagator, $\lim_{k\to 0}\Gamma^{(2)}_k(q)|_{\Phi=\langle\Phi\rangle}$, which formally receives contribu-

[7] In thermal equilibrium at high temperature this decoupling is not obvious. We will comment on this point in Sec. VI.

[8] We note that the expressions (2.7) obey the well known Gell-Mann–Oakes–Renner relation $m^2_\pi f^2_\pi = -2\hat{m}\langle\bar{\psi}\psi\rangle + \mathcal{O}(\hat{m}^2)$ [33].

tions from terms in Γ_k with arbitrarily high powers of derivatives and the expectation value σ_0. Realistic nonperturbative truncations of Γ_k which reduce the problem to a manageable size are crucial. We will follow here a twofold strategy:

Physical observables like meson masses, decay constants, etc., can be expanded in powers of (current) quark masses in a similar way as in chiral perturbation theory [34]. To a given finite order of this expansion only a finite number of terms of a simultaneous expansion of Γ_k in powers of derivatives and Φ are required if the expansion point is chosen properly. Details of this procedure and some results can be found in [35–37].

Because of an approximate partial IR fixed point behavior of the flow equations in the symmetric regime, i.e. for $k_{\chi SB}<k<k_\Phi$, the values of many parameters of Γ_k for $k\to 0$ will be almost independent of their initial values at the compositeness scale k_Φ. For large enough h_{k_Φ} only a few relevant parameters need to be computed accurately from QCD. They can alternatively be determined from phenomenology. Because of the present lack of an explicit QCD computation we will pursue the latter approach.

In combination, these two points open the possibility for a perhaps unexpected degree of predictive power within the linear quark meson model. We wish to stress, however, that a perturbative treatment of the model at hand, e.g., using perturbative RG techniques, cannot be expected to yield reliable results. The renormalized Yukawa coupling is very large at the scale k_Φ. Even the IR value of h_k is still relatively big

$$h_{k=0}=\frac{2M_q}{f_\pi}\simeq 6.5 \tag{2.9}$$

and h_k increases with k. The dynamics of the linear quark meson model is therefore clearly nonperturbative for all scales $k\leqslant k_\Phi$.

We will now turn to the flow equations for the linear quark meson model. We first note that the flow equations for Γ_k and $\Gamma_k-\frac{1}{2}\int d^4x\ \mathrm{tr}(J^\dagger\Phi+\Phi^\dagger J)$ are identical. The source term therefore does not need to be considered explicitly and only appears in the condition (2.5) for $\langle\Phi\rangle$. It is convenient to work with dimensionless and renormalized variables therefore eliminating all explicit k dependence. With

$$u(t,\tilde\rho)\equiv k^{-d}U_k(\rho),\quad \tilde\rho\equiv Z_{\Phi,k}k^{2-d}\rho \tag{2.10}$$

and using Eq. (1.6) as a first truncation of the effective average action Γ_k one obtains the flow equation [$t=\ln(k/k_\Phi)$]

$$\begin{aligned}\frac{\partial}{\partial t}u=&-du+(d-2+\eta_\Phi)\tilde\rho u'\\&+2v_d\Big\{3l_0^d(u';\eta_\Phi)+l_0^d(u'+2\tilde\rho u'';\eta_\Phi)\\&-2^{d/2+1}N_c l_0^{(F)d}\Big(\frac{1}{2}\tilde\rho h^2;\eta_\psi\Big)\Big\}.\end{aligned} \tag{2.11}$$

Here $v_d^{-1}\equiv 2^{d+1}\pi^{d/2}\Gamma(d/2)$ and primes denote derivatives with respect to $\tilde\rho$. The number of quark colors is denoted as N_c. We will always use in the following $N_c=3$. Equation (2.11) is a partial differential equation for the effective potential $u(t,\tilde\rho)$ which has to be supplemented by the flow equation for the Yukawa coupling and expressions for the anomalous dimensions η_Φ, η_ψ. The symbols l_n^d, $l_n^{(F)d}$ denote bosonic and fermionic mass threshold functions, respectively, which are defined in Appendix B. They describe the decoupling of massive modes and provide an important nonperturbative ingredient. For instance, the bosonic threshold functions

$$\begin{aligned}l_n^d(w;\eta_\Phi)=&\frac{n+\delta_{n,0}}{4}v_d^{-1}k^{2n-d}\int\frac{d^dq}{(2\pi)^d}\\&\times\frac{1}{Z_{\Phi,k}}\frac{\partial R_k}{\partial t}\frac{1}{[P(q^2)+k^2w]^{n+1}}\end{aligned} \tag{2.12}$$

involve the inverse average propagator $P(q^2)=q^2+Z_{\Phi,k}^{-1}R_k(q^2)$ where the infrared cutoff is manifest. These functions decrease $\sim w^{-(n+1)}$ for $w\gg 1$. Since typically $w=M^2/k^2$ with M a mass of the model, the main effect of the threshold functions is to cut off fluctuations of particles with masses $M^2\gg k^2$. Once the scale k is changed below a certain mass threshold, the corresponding particle no longer contributes to the evolution and decouples smoothly.

The dimensionless renormalized expectation value $\kappa\equiv 2k^{2-d}Z_{\Phi,k}\bar\sigma_{0,k}^2$, with $\bar\sigma_{0,k}$ the k-dependent VEV of Φ, may be computed for each k directly from the condition (2.5)

$$u'(t,\kappa)=\frac{J}{\sqrt{2\kappa}}k^{-(d+2)/2}Z_{\Phi,k}^{-1/2}\equiv\epsilon_g. \tag{2.13}$$

Note that $\kappa\equiv 0$ in the symmetric regime for vanishing source term. Equation (2.13) allows us to follow the flow of κ according to

$$\frac{d}{dt}\kappa=\frac{\kappa}{\epsilon_g+2\kappa\lambda}\left\{[\eta_\Phi-d-2]\epsilon_g-2\frac{\partial}{\partial t}u'(t,\kappa)\right\} \tag{2.14}$$

with $\lambda\equiv u''(t,\kappa)$. We define the Yukawa coupling for $\tilde\rho=\kappa$ and its flow equation reads [27]

$$\frac{d}{dt}h^2=(d-4+2\eta_\psi+\eta_\Phi)h^2 - 2v_d h^4\left\{3l_{1,1}^{(FB)d}\left(\frac{1}{2}h^2\kappa,\epsilon_g;\eta_\psi,\eta_\Phi\right) - l_{1,1}^{(FB)d}\left(\frac{1}{2}h^2\kappa,\epsilon_g+2\lambda\kappa;\eta_\psi,\eta_\Phi\right)\right\}. \quad (2.15)$$

Similarly, the scalar and quark anomalous dimensions are inferred from

$$\eta_\Phi\equiv-\frac{d}{dt}\ln Z_{\Phi,k} =4\frac{v_d}{d}\left\{4\kappa\lambda^2 m_{2,2}^d(\epsilon_g,\epsilon_g+2\lambda\kappa;\eta_\Phi) +2^{d/2}N_c h^2 m_4^{(F)d}\left(\frac{1}{2}h^2\kappa;\eta_\psi\right)\right\},$$

$$\eta_\psi\equiv-\frac{d}{dt}\ln Z_{\psi,k} =2\frac{v_d}{d}h^2\left\{3m_{1,2}^{(FB)d}\left(\frac{1}{2}h^2\kappa,\epsilon_g;\eta_\psi,\eta_\Phi\right) + m_{1,2}^{(FB)d}\left(\frac{1}{2}h^2\kappa,\epsilon_g+2\lambda\kappa;\eta_\psi,\eta_\Phi\right)\right\}, \quad (2.16)$$

which is a linear set of equations for the anomalous dimensions. The threshold functions $l_{n_1,n_2}^{(FB)d}$, m_{n_1,n_2}^d, $m_4^{(F)d}$ and $m_{n_1,n_2}^{(FB)d}$ are also specified in Appendix B.

The flow equations (2.11), (2.14)–(2.16), constitute a coupled system of ordinary and partial differential equations which can be integrated numerically. Here we take the effective current quark mass dependence of h_k, $Z_{\Phi,k}$ and $Z_{\psi,k}$ into account by stopping the evolution according to Eqs. (2.15), (2.16), evaluated for the chiral limit, below the pion mass m_π. (For details of the algorithm used here see Refs. [38, 39].) One finds for $d=4$ that chiral symmetry breaking indeed occurs for a wide range of initial values of the parameters including the presumably realistic case of large renormalized Yukawa coupling and a bare mass $\bar{m}_{k_\Phi}$ of order 100 MeV. Driven by the strong Yukawa coupling, the renormalized mass term $u'(t,\tilde{\rho}=0)$ decreases rapidly and goes through zero at a scale $k_{\chi\mathrm{SB}}$ not far below k_Φ. Here the system enters the spontaneously broken regime and the effective average potential develops an absolute minimum away from the origin. The evolution of the potential minimum $\sigma_{0,k}^2=k^2\kappa/2$ turns out to be reasonably stable already before $k\simeq m_\pi$ where it stops. We take this result as an indication that our truncation of the effective action Γ_k leads at least qualitatively to a satisfactory description of chiral symmetry breaking. The reason for the relative stability of the IR behavior of the VEV (and all other couplings) is that the quarks acquire a constituent mass $M_q=h\sigma_0\simeq 300$ MeV in the spontaneously broken regime. As a consequence they decouple once k becomes smaller than M_q and the evolution is then dominantly driven by the light Goldstone bosons. This is also important for our approximation of neglecting the residual gluonic interactions in the quark sector of the model as outlined in Sec. II A.

Most importantly, one finds that the system of flow equations exhibits an approximate IR fixed point behavior in the symmetric regime [27]. To see this explicitly we study the flow equations (2.11), (2.14)–(2.16) subject to the condition (2.2). For the relevant range of $\tilde{\rho}$ both $u'(t,\tilde{\rho})$ and $u'(t,\tilde{\rho})+2\tilde{\rho}u''(t,\tilde{\rho})$ are then much larger than $\tilde{\rho}h^2(t)$ and we may therefore neglect in the flow equations all scalar contributions with threshold functions involving these large masses. This yields the simplified equations ($d=4$, $v_4^{-1}=32\pi^2$)

$$\frac{\partial}{\partial t}u=-4u+(2+\eta_\Phi)\tilde{\rho}u'-\frac{N_c}{2\pi^2}l_0^{(F)4}\left(\frac{1}{2}\tilde{\rho}h^2\right),$$

$$\frac{d}{dt}h^2=\eta_\Phi h^2,$$

$$\eta_\Phi=\frac{N_c}{8\pi^2}m_4^{(F)4}(0)h^2,$$

$$\eta_\psi=0. \quad (2.17)$$

Of course, it should be clear that this approximation is only valid for the initial range of running below k_Φ before the (dimensionless) renormalized scalar mass squared $u'(t,\tilde{\rho}=0)$ approaches zero near the chiral symmetry breaking scale. The system (2.17) is exactly soluble. Using $m_4^{(F)4}(0)=1$ which holds independently of the choice of the IR cutoff we find

$$h^2(t)=Z_\Phi^{-1}(t)=\frac{h_I^2}{1-\frac{N_c}{8\pi^2}h_I^2 t},$$

$$u(t,\tilde{\rho})=e^{-4t}u_I\left(e^{2t}\tilde{\rho}\,\frac{h^2(t)}{h_I^2}\right) -\frac{N_c}{2\pi^2}\int_0^t dr e^{-4r}l_0^{(F)4}\left(\frac{1}{2}h^2(t)\tilde{\rho}e^{2r}\right). \quad (2.18)$$

[The integration over r on the right hand side of the solution for u can be carried out by first exchanging it with the one over momentum implicit in the definition of the threshold function $l_0^{(F)4}$ (see Appendix B).] Here $u_I(\tilde{\rho})\equiv u(0,\tilde{\rho})$ denotes the effective average potential at the compositeness scale and h_I^2 is the initial value of h^2 at k_Φ, i.e. for $t=0$. For simplicity we will use an expansion of the initial value effective potential $u_I(\tilde{\rho})$ in powers of $\tilde{\rho}$ around $\tilde{\rho}=0$

$$u_I(\tilde{\rho})=\sum_{n=0}^{\infty}\frac{u_I^{(n)}(0)}{n!}\tilde{\rho}^n \quad (2.19)$$

TABLE II. The table shows the dependence on the constituent quark mass M_q of the input parameters k_Φ, $\bar{m}^2_{k_\Phi}/k^2_\Phi$ and J as well as some of our ''predictions.'' The phenomenological input used here besides M_q is $f_\pi = 92.4$ MeV, $m_\pi = 135$ MeV. The first line corresponds to the values for M_q and λ_I used in the remainder of this work. The other three lines demonstrate the insensitivity of our results with respect to the precise values of these parameters.

$\frac{M_q}{\text{MeV}}$	$\frac{\lambda_I}{h_I^2}$	$\frac{k_\Phi}{\text{MeV}}$	$\frac{\bar{m}^2_{k_\Phi}}{k^2_\Phi}$	$\frac{J^{1/3}}{\text{MeV}}$	$\frac{\hat{m}(k_\Phi)}{\text{MeV}}$	$\frac{\hat{m}(1\text{ GeV})}{\text{MeV}}$	$\frac{\langle\bar{\psi}\psi\rangle(1\text{ GeV})}{\text{MeV}^3}$	$\frac{f_\pi^{(0)}}{\text{MeV}}$
303	1	618	0.0265	66.8	14.7	11.4	$-(186)^3$	80.8
300	0	602	0.026	66.8	15.8	12.0	$-(183)^3$	80.2
310	0	585	0.025	66.1	16.9	12.5	$-(180)^3$	80.5
339	0	552	0.0225	64.4	19.5	13.7	$-(174)^3$	81.4

even though this is not essential for the forthcoming reasoning. Expanding also $l_0^{(F)4}$ in Eq. (2.18) in powers of its argument one finds for $n>2$

$$\frac{u^{(n)}(t,0)}{h^{2n}(t)} = e^{2(n-2)t}\frac{u_I^{(n)}(0)}{h_I^{2n}} + \frac{N_c}{\pi^2}\frac{(-1)^n(n-1)!}{2^{n+2}(n-2)} l_n^{(F)4}(0) \times [1-e^{2(n-2)t}]. \tag{2.20}$$

For decreasing $t\to-\infty$ the initial values $u_I^{(n)}$ become rapidly unimportant and $u^{(n)}/h^{2n}$ approaches a fixed point. For $n=2$, i.e., for the quartic coupling, one finds

$$\frac{u^{(2)}(t,0)}{h^2(t)} = 1 - \frac{1-\dfrac{u_I^{(2)}(0)}{h_I^2}}{1-\dfrac{N_c}{8\pi^2}h_I^2 t} \tag{2.21}$$

leading to a fixed point value $(u^{(2)}/h^2)_* = 1$. As a consequence of this fixed point behavior the system loses all its ''memory'' on the initial values $u_I^{(n\geq 2)}$ at the compositeness scale k_Φ. This typically happens before the approximation $u'(t,\tilde{\rho}), u'(t,\tilde{\rho}) + 2\tilde{\rho}u''(t,\tilde{\rho}) \gg \tilde{\rho}h^2(t)$ breaks down and the solution (2.18) becomes invalid. Furthermore, the attraction to partial infrared fixed points continues also for the range of k where the scalar fluctuations cannot be neglected anymore. The initial value for the bare dimensionless mass parameter

$$\frac{u_I'(0)}{h_I^2} = \frac{\bar{m}^2_{k_\Phi}}{k^2_\Phi} \tag{2.22}$$

is never negligible. (In fact, using the values for $\bar{m}^2_{k_\Phi}$ and k_Φ computed in Ref. [26] one obtains $\bar{m}^2_{k_\Phi}/k^2_\Phi \simeq 0.036$.) For large h_I [and dropping the constant piece $u_I(0)$] the solution (2.18) therefore behaves with growing $|t|$ as

$$Z_\Phi(t) \simeq -\frac{N_c}{8\pi^2}t,$$

$$h^2(t) \simeq -\frac{8\pi^2}{N_c t},$$

$$u(t,\tilde{\rho}) \simeq \frac{u_I'(0)}{h_I^2}e^{-2t}h^2(t)\tilde{\rho} - \frac{N_c}{2\pi^2} \times \int_0^t dr e^{-4r} l_0^{(F)4}\left(\frac{1}{2}h^2(t)\tilde{\rho}e^{2r}\right). \tag{2.23}$$

In other words, for $h_I\to\infty$ the IR behavior of the linear quark meson model will depend (in addition to the value of the compositeness scale k_Φ and the quark mass $\hat{m}$) only on one parameter, $\bar{m}^2_{k_\Phi}$. We have numerically verified this feature by starting with different values for $u_I^{(2)}(0)$. Indeed, the differences in the physical observables were found to be small. This IR stability of the flow equations leads to a perhaps surprising degree of predictive power. For definiteness we will perform our numerical analysis of the full system of flow equations (2.11), (2.14)–(2.16) with the idealized initial value $u_I(\tilde{\rho}) = u_I'(0)\tilde{\rho}$ in the limit $h_I^2\to\infty$. It should be stressed, though, that deviations from this idealization will lead only to small numerical deviations in the IR behavior of the linear quark meson model as long as the condition (2.2) holds, say for $h_I \gtrsim 15$ [27].

With this knowledge at hand we may now fix the remaining three parameters of our model, k_Φ, $\bar{m}^2_{k_\Phi}$ and $\hat{m}$ by using $f_\pi = 92.4$ MeV, the pion mass $M_\pi = 135$ MeV and the constituent quark mass M_q as phenomenological input. Because of the uncertainty regarding the precise value of M_q we give in Table II the results for several values of M_q. The first line of Table II corresponds to the choice of M_q and $\lambda_I \equiv u_I''(\kappa)$ which we will use for the forthcoming analysis of the model at finite temperature. As argued analytically above the dependence on the value of λ_I is weak for large enough h_I as demonstrated numerically by the second line. Moreover, we notice that our results, and in particular the value of J, are rather insensitive with respect to the precise value of M_q. It is remarkable that the values for k_Φ and $\bar{m}_{k_\Phi}$ are not very different from those computed in Ref. [26]. As compared to the analysis of Ref. [27] the present truncation of Γ_k is of a higher level of accuracy: We now consider an arbitrary form of the effective average potential instead of a polynomial approximation and we have included the pieces in the threshold functions which are proportional to the anomalous dimensions. It is encouraging that the results are rather robust with respect to these improvements of the truncation.

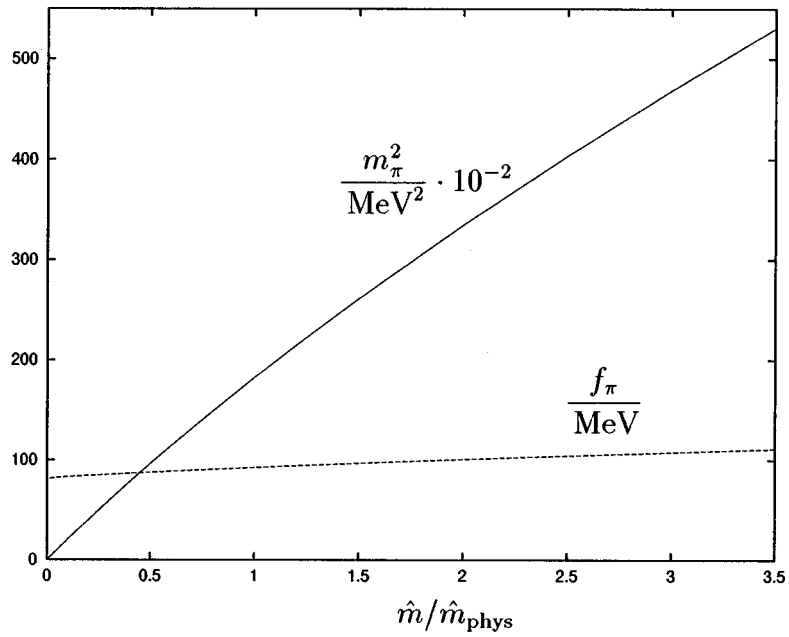

FIG. 4. The plot shows m_π^2 (solid line) and f_π (dashed line) as functions of the current quark mass $\hat{m}$ in units of the physical value $\hat{m}_{\mathrm{phys}}$.

Once the parameters k_Φ, $\bar{m}^2_{k_\Phi}$ and $\hat{m}$ are fixed there are a number of ''predictions'' of the linear meson model which can be compared with the results obtained by other methods or direct experimental observation. First of all one may compute the value of $\hat{m}$ at a scale of 1 GeV which is suitable for comparison with results obtained from chiral perturbation theory [40] and sum rules [41]. For this purpose one has to account for the running of this quantity with the normalization scale from k_Φ as given in Table II to the commonly used value of 1 GeV: $\hat{m}(1\ \mathrm{GeV})=A^{-1}\hat{m}(k_\Phi)$. A reasonable estimate of the factor A is obtained from the three loop running of $\hat{m}$ in the modified minimal subtraction ($\overline{\mathrm{MS}}$) scheme [41]. For $M_q\simeq 300$ MeV corresponding to the first two lines in Table II its value is $A\simeq 1.3$. The results for $\hat{m}(1\ \mathrm{GeV})$ are in acceptable agreement with recent results from other methods [40,41] even though they tend to be somewhat larger. Closely related to this is the value of the chiral condensate

$$\langle\bar{\psi}\psi\rangle(1\ \mathrm{GeV})\equiv -A\bar{m}^2_{k_\Phi}[f_\pi Z^{-1/2}_{\Phi,k=0}-2\hat{m}]. \qquad (2.24)$$

These results are quite non-trivial since not only f_π and $\bar{m}^2_{k_\Phi}$ enter but also the computed IR value $Z_{\Phi,k=0}$. We emphasize in this context that there may be substantial corrections both in the extrapolation from k_Φ to 1 GeV and in the factor a_q [see Eq. (A1)]. The latter is due to the neglected influence of the strange quark which may be important near k_Φ. These uncertainties have only little effect on the physics at lower scales as relevant for our analysis of the temperature effects. Only the value of J which is fixed by m_π enters here.

A further more qualitative test concerns the mass of the sigma resonance or radial mode whose renormalized mass squared may be computed according to Eq. (2.7) in the limit $k\to 0$. From our numerical analysis we obtain $\lambda_{k=0}\simeq 20$ which translates into $m_\sigma\simeq 430$ MeV. One should note, though, that this result is presumably not very accurate as we have employed in this work the approximation of using the Goldstone boson wave function renormalization constant also for the radial mode. Furthermore, the explicit chiral symmetry breaking contribution to m_σ^2 is certainly underestimated as long as the strange quark is neglected. In any case, we observe that the sigma meson is significantly heavier than the pions. This is a crucial consistency check for the linear quark meson model. A low sigma mass would be in conflict with the numerous successes of chiral perturbation theory [34] which requires the decoupling of all modes other than the Goltone bosons in the IR limit of QCD. The decoupling of the sigma meson is, of course, equivalent to the limit $\lambda\to\infty$ which formally describes the transition from the linear to the non-linear sigma model and which appears to be reasonably well realized by the large IR values of λ obtained in our analysis. We also note that the issue of the sigma mass is closely connected to the value of $f_\pi^{(0)}$, the value of f_π in the chiral limit $\hat{m}=0$ also given in Table II. To lowest order in $(f_\pi-f_\pi^{(0)})/f_\pi$ or, equivalently, in $\hat{m}$ one has

$$f_\pi-f_\pi^{(0)}=\frac{J}{Z_\Phi^{1/2}m_\sigma^2}=\frac{f_\pi m_\pi^2}{m_\sigma^2}. \qquad (2.25)$$

A larger value of m_σ would therefore reduce the difference between $f_\pi^{(0)}$ and f_π.

In Fig. 4 we show the dependence of the pion mass and decay constant on the average current quark mass $\hat{m}$. These curves depend very little on the values of the initial parameters as demonstrated in Table II by $f_\pi^{(0)}$. We observe a relatively large difference of 12 MeV between the pion decay constants at $\hat{m}=\hat{m}_{\mathrm{phys}}$ and $\hat{m}=0$. According to Eq. (2.25) this difference is related to the mass of the sigma particle and will be modified in the three flavor case. We will

later find that the critical temperature T_c for the second order phase transition in the chiral limit is almost independent of the initial conditions. The values of $f_\pi^{(0)}$ and T_c essentially determine the non-universal amplitudes in the critical scaling region (cf. Sec. V). In summary, we find that the behavior of our model for small k is quite robust as far as uncertainties in the initial conditions at the scale k_Φ are concerned. We will see that the difference of observables between non-vanishing and vanishing temperature is entirely determined by the flow of couplings in the range $0<k\lesssim 3T$.

III. THERMAL EQUILIBRIUM AND DIMENSIONAL REDUCTION

The extension of flow equations to thermal equilibrium situations at non-vanishing temperature T is straightforward [42]. In the Euclidean formalism non-zero temperature results in (anti-)periodic boundary conditions for (fermionic) bosonic fields in the Euclidean time direction with periodicity $1/T$ [43]. This leads to the replacement

$$\int \frac{d^d q}{(2\pi)^d} f(q^2) \to T\sum_{l\in\mathbb{Z}} \int \frac{d^{d-1}\vec{q}}{(2\pi)^{d-1}} f(q_0^2(l)+\vec{q}^2) \tag{3.1}$$

in the trace in Eq. (1.1) when represented as a momentum integration, with a discrete spectrum for the zero component

$$q_0(l)=\begin{cases} 2l\pi T & \text{for bosons,} \\ (2l+1)\pi T & \text{for fermions.} \end{cases} \tag{3.2}$$

Hence, for $T>0$ a four-dimensional QFT can be interpreted as a three-dimensional model with each bosonic or fermionic degree of freedom now coming in an infinite number of copies labeled by $l\in\mathbb{Z}$ (Matsubara modes). Each mode acquires an additional temperature dependent effective mass term $q_0^2(l)$. In a high temperature situation where all massive Matsubara modes decouple from the dynamics of the system one therefore expects to observe an effective three-dimensional theory with the bosonic zero modes as the only relevant degrees of freedom. In other words, if the characteristic length scale associated with the physical system is much larger than the inverse temperature the compactified Euclidean ''time'' dimension cannot be resolved anymore. This phenomenon is known as ''dimensional reduction'' [44].

The formalism of the effective average action automatically provides the tools for a smooth decoupling of the massive Matsubara modes as the scale k is lowered from $k\gg T$ to $k\ll T$. It therefore allows us to directly link the low-T, four-dimensional QFT to the effective three-dimensional high-T theory. The replacement (3.1) in (1.1) manifests itself in the flow equations (2.11), (2.14)–(2.16) only through a change to T-dependent threshold functions. For instance, the dimensionless functions $l_n^d(w;\eta_\Phi)$ defined in Eq. (2.12) are replaced by

$$l_n^d\left(w,\frac{T}{k};\eta_\Phi\right) \equiv \frac{n+\delta_{n,0}}{4} v_d^{-1} k^{2n-d} T\sum_{l\in\mathbb{Z}} \int \frac{d^{d-1}\vec{q}}{(2\pi)^{d-1}} \times\left(\frac{1}{Z_{\Phi,k}}\frac{\partial R_k(q^2)}{\partial t}\right)\frac{1}{[P(q^2)+k^2 w]^{n+1}} \tag{3.3}$$

where $q^2=q_0^2+\vec{q}^2$ and $q_0=2\pi l T$. A list of the various temperature dependent threshold functions appearing in the flow equations can be found in Appendix C. There we also discuss some subtleties regarding the definition of the Yukawa coupling and the anomalous dimensions for $T\neq 0$. In the limit $k\gg T$ the sum over Matsubara modes approaches the integration over a continuous range of q_0 and we recover the zero temperature threshold function $l_n^d(w;\eta_\Phi)$. In the opposite limit $k\ll T$ the massive Matsubara modes ($l\neq 0$) are suppressed and we expect to find a $d-1$ dimensional behavior of l_n^d. In fact, one obtains from Eq. (3.3)

$$l_n^d(w,T/k;\eta_\Phi)\simeq l_n^d(w;\eta_\Phi) \quad \text{for } T\ll k,$$
$$l_n^d(w,T/k;\eta_\Phi)\simeq \frac{T}{k}\frac{v_{d-1}}{v_d} l_n^{d-1}(w;\eta_\Phi) \quad \text{for } T\gg k. \tag{3.4}$$

For our choice of the infrared cutoff function R_k, Eq. (1.3), the temperature dependent Matsubara modes in $l_n^d(w,T/k;\eta_\Phi)$ are exponentially suppressed for $T\ll k$ whereas the behavior is more complicated for other threshold functions appearing in the flow equations (2.11), (2.14)–(2.16). Nevertheless, all bosonic threshold functions are proportional to T/k for $T\gg k$ whereas those with fermionic contributions vanish in this limit.[9] This behavior is demonstrated in Fig. 5 where we have plotted the quotients $l_1^4(w,T/k)/l_1^4(w)$ and $l_1^{(F)4}(w,T/k)/l_1^{(F)4}(w)$ of bosonic and fermionic threshold functions, respectively. One observes that for $k\gg T$ both threshold functions essentially behave as for zero temperature. For growing T or decreasing k this changes as more and more Matsubara modes decouple until finally all massive modes are suppressed. The bosonic threshold function l_1^4 shows for $k\ll T$ the linear dependence on T/k derived in Eq. (3.4). In particular, for the bosonic excitations the threshold function for $w\ll 1$ can be approximated with reasonable accuracy by $l_n^4(w;\eta_\Phi)$ for $T/k<0.25$ and by $(4T/k)l_n^3(w;\eta_\Phi)$ for $T/k>0.25$. The fermionic threshold function $l_1^{(F)4}$ ten to zero for $k\ll T$ since there is no massless fermionic zero mode, i.e., in this limit all fermionic contributions to the flow equations are suppressed. On the other hand, the fermions remain quantitatively relevant up to $T/k\simeq 0.6$ because of the relatively long tail in Fig. 5(b). The transition from four to three-dimensional threshold functions leads to a *smooth dimensional reduction* as k is lowered from $k\gg T$ to $k\ll T$. Whereas for $k\gg T$ the

[9]For the present choice of R_k the temperature dependence of the threshold functions is considerably smoother than in Ref. [42].

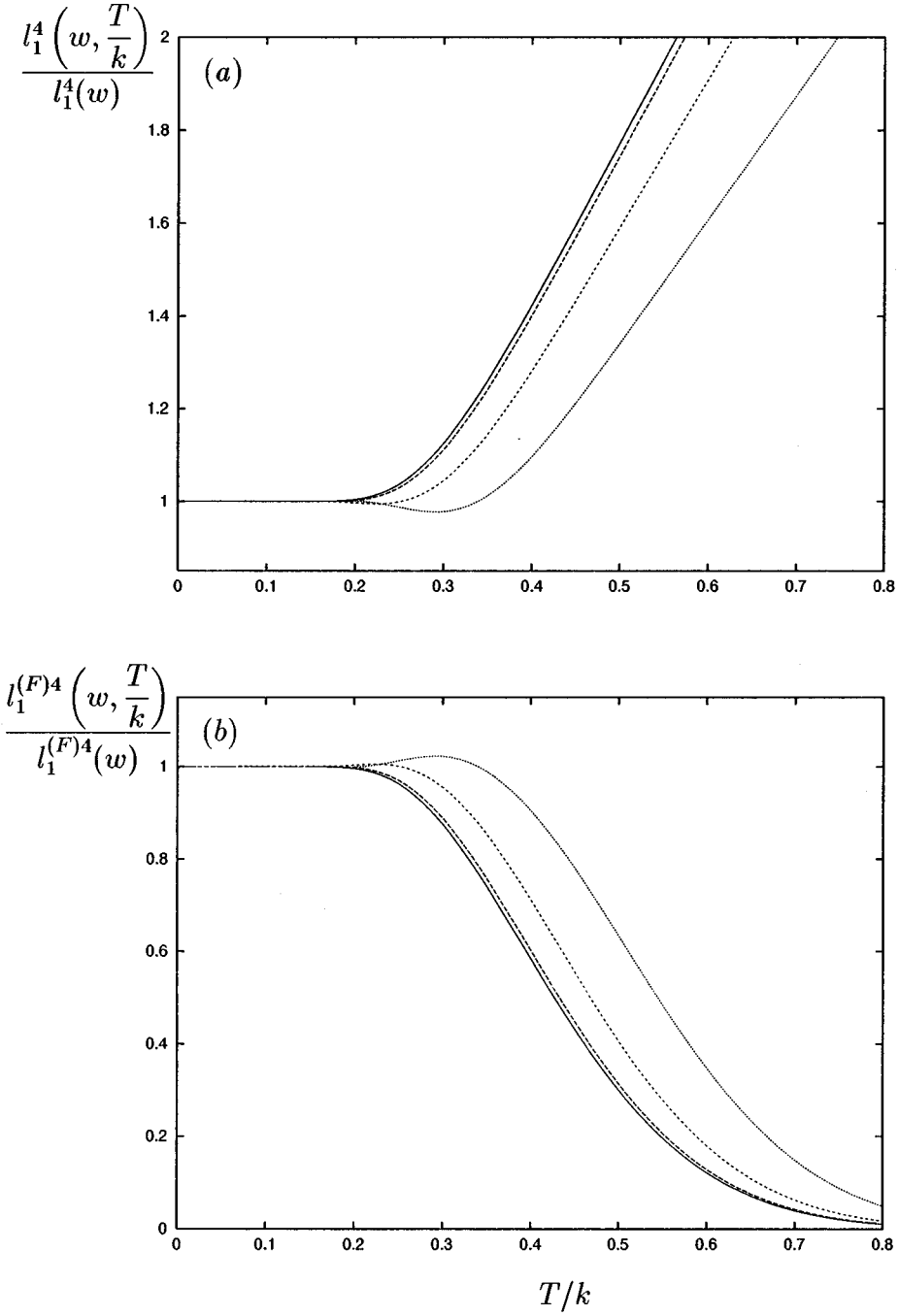

FIG. 5. The plot shows the temperature dependence of the bosonic (a) and the fermionic (b) threshold functions $l_1^4(w,T/k)$ and $l_1^{(F)4}(w,T/k)$, respectively, for different values of the dimensionless mass term w. The solid line corresponds to $w=0$ whereas the dotted ones correspond to $w=0.1$, $w=1$ and $w=10$ with decreasing size of the dots. For $T\gg k$ the bosonic threshold function becomes proportional to T/k whereas the fermionic one ten to zero. In this range the theory with properly rescaled variables behaves as a classical three-dimensional theory.

model is most efficiently described in terms of standard four-dimensional fields Φ a choice of rescaled three-dimensional variables $\Phi_3=\Phi/\sqrt{T}$ becomes better adapted for $k\ll T$. Accordingly, for high temperatures one will use a potential

$$u_3(t,\tilde{\rho}_3)=\frac{k}{T}u(t,\tilde{\rho});\quad \tilde{\rho}_3=\frac{k}{T}\tilde{\rho}. \tag{3.5}$$

In this regime $\Gamma_{k\to 0}$ corresponds to the free energy of classical statistics and $\Gamma_{k>0}$ is a classical coarse grained free energy.

For our numerical calculations at non-vanishing temperature we exploit the discussed behavior of the threshold functions by using the zero temperature flow equations in the range $k\geqslant 10T$. For smaller values of k we approximate the

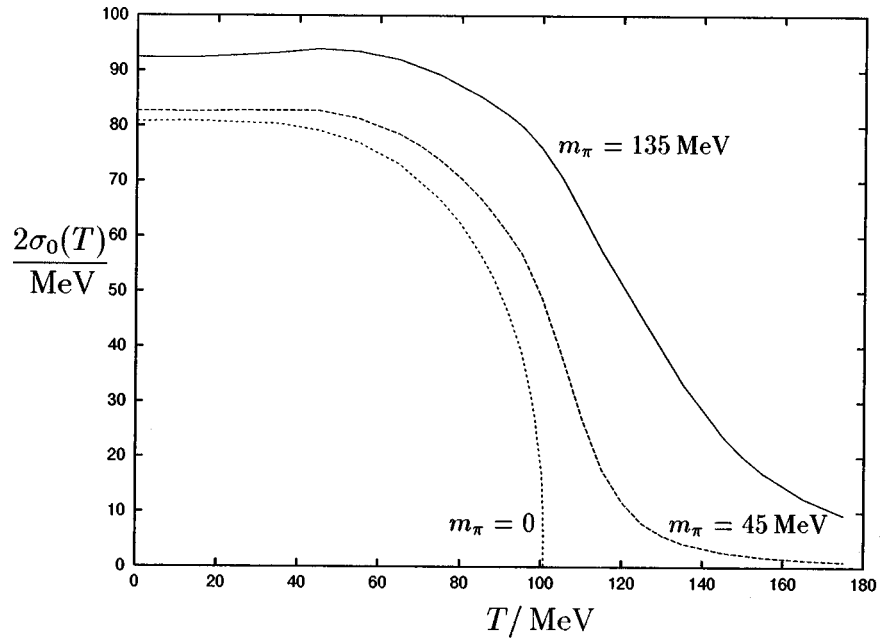

FIG. 6. The expectation value $2\sigma_0$ is shown as a function of temperature T for three different values of the zero temperature pion mass.

infinite Matsubara sums [cf. Eq. (3.3)] by a finite series such that the numerical uncertainty at $k=10T$ is better than 10^{-4}. This approximation becomes exact in the limit $k \ll 10T$.

IV. THE QUARK MESON MODEL AT $T \neq 0$

In Sec. II A we have considered the relevant fluctuations that contribute to the flow of Γ_k in dependence on the scale k. In a thermal equilibrium situation Γ_k also depends on the temperature T and one may ask for the relevance of thermal fluctuations at a given scale k. In particular, for not too high values of T (cf. Sec. VI) the ''initial condition'' Γ_{k_Φ} for the solution of the flow equations should essentially be independent of temperature. This will allow us to fix Γ_{k_Φ} from phenomenological input at $T=0$ and to compute the temperature dependent quantities in the infrared $(k \to 0)$. We note that the thermal fluctuations which contribute to the right-hand side of the flow equation for the meson potential (2.11) are effectively suppressed for $T \lesssim k/4$ (cf. Sec. III). Clearly for $T \gtrsim k_\Phi/3$ temperature effects become important at the compositeness scale. We expect the linear quark meson model with a compositeness scale $k_\Phi \simeq 600$ MeV to be a valid description for two flavor QCD below a temperature of about[10] 170 MeV.

We compute the quantities of interest for temperatures $T \lesssim 170$ MeV by solving numerically the T-dependent version of the flow equations (2.11), (2.14)–(2.16) (cf. Sec. III and Appendix C) by lowering k from k_Φ to zero. For this range of temperatures we use the initial values as given in the first line of Table II. This corresponds to choosing the zero temperature pion mass and the pion decay constant ($f_\pi = 92.4$ MeV for $m_\pi = 135$ MeV) as phenomenological input. The only further input is the constituent quark mass M_q which we vary in the range $M_q \simeq 300$–350 MeV. We observe only a minor dependence of our results on M_q for the considered range of values. In particular, the value for the critical temperature T_c of the model remains almost unaffected by this variation.

We have plotted in Fig. 6 the renormalized expectation value $2\sigma_0$ of the scalar field as a function of temperature for three different values of the average light current quark mass $\hat{m}$. [We remind that $2\sigma_0(T=0) = f_\pi$.] For $\hat{m}=0$ the order parameter σ_0 of chiral symmetry breaking continuously goes to zero for $T \to T_c = 100.7$ MeV characterizing the phase transition to be of second order. The universal behavior of the model for small $T - T_c$ and small $\hat{m}$ is discussed in more detail in Sec. V. We point out that the value of T_c corresponds to $f_\pi^{(0)} = 80.8$ MeV, i.e. the value of the pion decay constant for $\hat{m}=0$, which is significantly lower than $f_\pi = 92.4$ MeV obtained for the realistic value $\hat{m}_{\text{phys}}$. If we would fix the value of the pion decay constant to be 92.4 MeV also in the chiral limit $(\hat{m}=0)$, the value for the critical temperature would raise to 115 MeV. The nature of the transition changes qualitatively for $\hat{m} \neq 0$ where the second order transition is replaced by a smooth crossover. The crossover for a realistic $\hat{m}_{\text{phys}}$ or $m_\pi(T=0) = 135$ MeV takes place in a temperature range $T \simeq (120$–$150)$ MeV. The middle curve in Fig. 6 corresponds to a value of $\hat{m}$ which is only a tenth of the physical value, leading to a zero temperature pion mass $m_\pi = 45$ MeV. Here the crossover becomes considerably

[10]There will be an effective temperature dependence of Γ_{k_Φ} induced by the fluctuations of other degrees of freedom besides the quarks, the pions and the sigma which are taken into account here. We will comment on this issue in Sec. VI. For realistic three flavor QCD the thermal kaon fluctuations will become important for $T \gtrsim 170$ MeV.

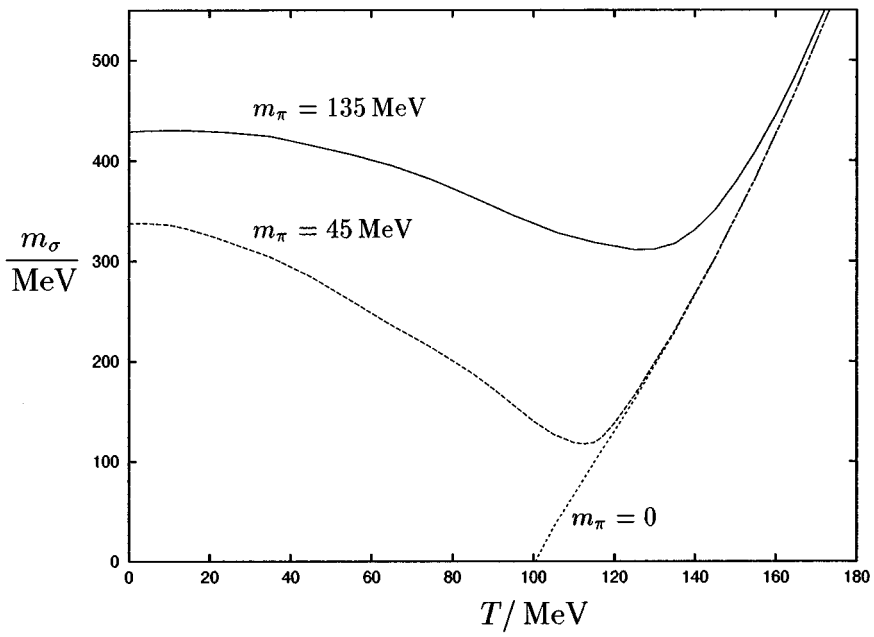

FIG. 7. The plot shows the m_σ as a function of temperature T for three different values of the zero temperature pion mass.

sharper but there remain substantial deviations from the chiral limit even for such small quark masses $\hat{m} \simeq 1$ MeV. The temperature dependence of m_π has already been mentioned in the Introduction (see Fig. 2) for the same three values of $\hat{m}$. As expected, the pions behave like true Goldstone bosons for $\hat{m}=0$, i.e. their mass vanishes for $T \leqslant T_c$. Interestingly, m_π remains almost constant as a function of T for $T<T_c$ before it starts to increase monotonically. We therefore find for two flavors no indication for a substantial decrease of m_π around the critical temperature.

The dependence of the mass of the sigma resonance m_σ on the temperature is displayed in Fig. 7 for the above three values of $\hat{m}$. In the absence of explicit chiral symmetry breaking, $\hat{m}=0$, the sigma mass vanishes for $T \leqslant T_c$. For $T<T_c$ this is a consequence of the presence of massless Goldstone bosons in the Higgs phase which drive the renormalized quartic coupling λ to zero. In fact, λ runs linearly with k for $T \gtrsim k/4$ and only evolves logarithmically for $T \lesssim k/4$. Once $\hat{m} \neq 0$ the pions acquire a mass even in the spontaneously broken phase and the evolution of λ with k is effectively stopped at $k \sim m_\pi$. Because of the temperature dependence of $\sigma_{0,k=0}$ (cf. Fig. 6) this leads to a monotonically decreasing behavior of m_σ with T for $T \lesssim T_c$. This changes into the expected monotonic growth once the system reaches the symmetric phase for[11] $T>T_c$. For low enough $\hat{m}$ one may use the minimum of $m_\sigma(T)$ for an alternative definition of the (pseudo-)critical temperature denoted as $T_{pc}^{(2)}$. Table I in the Introduction shows our results for the pseudocritical temperature for different values of $\hat{m}$ or, equivalently, $m_\pi(T=0)$. For a zero temperature pion mass $m_\pi = 135$ MeV we find $T_{pc}^{(2)}=128$ MeV. At larger pion masses of about 230 MeV we observe no longer a characteristic minimum for m_σ apart from a very broad, slight dip at $T \simeq 90$ MeV. A comparison of our results with lattice data is given in Sec. V. In Fig. 8 we show the renormalized quartic coupling λ as a function of temperature for two fixed values of the average current quark mass. The upper curve corresponds to the physical value of $\hat{m}$ or, equivalently, $m_\pi(T=0)=135$ MeV whereas the lower curve shows λ for $\hat{m}=0$. One observes the vanishing of the renormalized quartic coupling in the chiral limit for $T \leqslant T_c$ as discussed above. The renormalized scalar Φ^6 self interaction

$$U_3(T) = Z_\Phi^{-3} \frac{\partial^3 U(\rho,T)}{\partial \rho^3}(\rho = 2\bar{\sigma}_0^2(T)) \tag{4.1}$$

assumes a small negative value for realistic quark masses in the temperature range $T \lesssim 35$ MeV with $2U_3(T)\sigma_0^2(T) \simeq -0.5 \ll \lambda(T)$ and $2U_3(T)\sigma_0^2(T) \simeq 8.0, 8.5, 1.5$ for $T=80,120,160$ MeV. We display $U_3(T)$ in Fig. 9 for the chiral limit where one observes a discontinuity of $U_3(T)$ at the critical temperature T_c.

Our results for the chiral condensate $\langle \bar{\psi}\psi \rangle$ as a function of temperature for different values of the average current quark mass are presented in Fig. 1 in the Introduction. We will compare $\langle \bar{\psi}\psi \rangle(T,\hat{m})$ with its universal scaling form for the $O(4)$ Heisenberg model in Sec. V. Another interesting quantity is the temperature dependence of the constituent quark mass. Figure 10 shows $M_q(T)$ for $\hat{m}=0$, $\hat{m}=\hat{m}_{\text{phys}}/10$ and $\hat{m}=\hat{m}_{\text{phys}}$, respectively. Its behavior is related to the temperature dependence of the renormalized order parameter $\sigma_0(T) \equiv \sigma_{0,k=0}(T)$ and the renormalized Yukawa coupling $h(T) \equiv h_{k=0}(T)$. The temperature depen-

[11]See Sec. II B for a discussion of the zero temperature sigma mass.

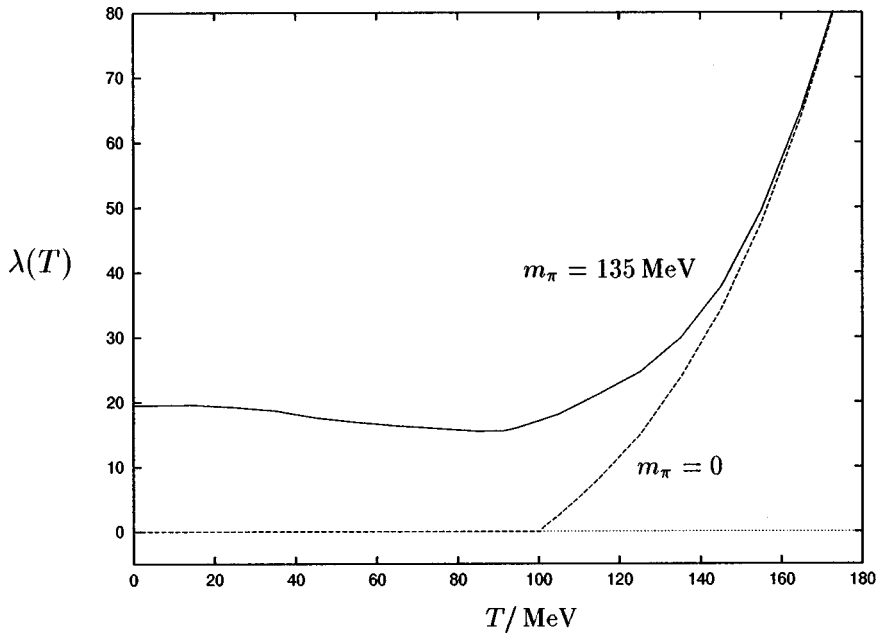

FIG. 8. The plot shows the renormalized quartic scalar self coupling λ as a function of temperature T for the physical value of $\hat{m}$ (solid line) as well as for $\hat{m}=0$ (dashed line).

dence of h in the chiral limit can be found in Fig. 11. Near the critical temperature one notices a characteristic dip. This results from the long wavelength pion fluctuations through a non-analytic behavior of the mesonic wave function renormalization $Z_\Phi(T) \equiv Z_{\Phi,k=0}(T)$ which is displayed in Fig. 12. There we also present the temperature dependence of the fermionic wave function renormalization $Z_\psi(T) \equiv Z_{\psi,k=0}(T)$. Away from the chiral limit we take the effective quark mass dependence of $h_k(T)$, $Z_{\Phi,k}(T)$ and $Z_{\psi,k}(T)$ into account by stopping their evolution when k reaches the temperature dependent pion mass. In this way we observe no substantial quark mass dependence of these quantities except for $Z_\Phi(T)$, and consequently for $h(T)$, in the vicinity of the critical temperature. A more complete truncation would incorporate field dependent wave function renormalization constants and a field dependent Yukawa coupling.

Our ability to compute the complete temperature dependent effective meson potential U is demonstrated in Fig. 13 where we display the derivative of the potential with respect to the renormalized field $\phi_R = (Z_\Phi \rho/2)^{1/2}$, for different val-

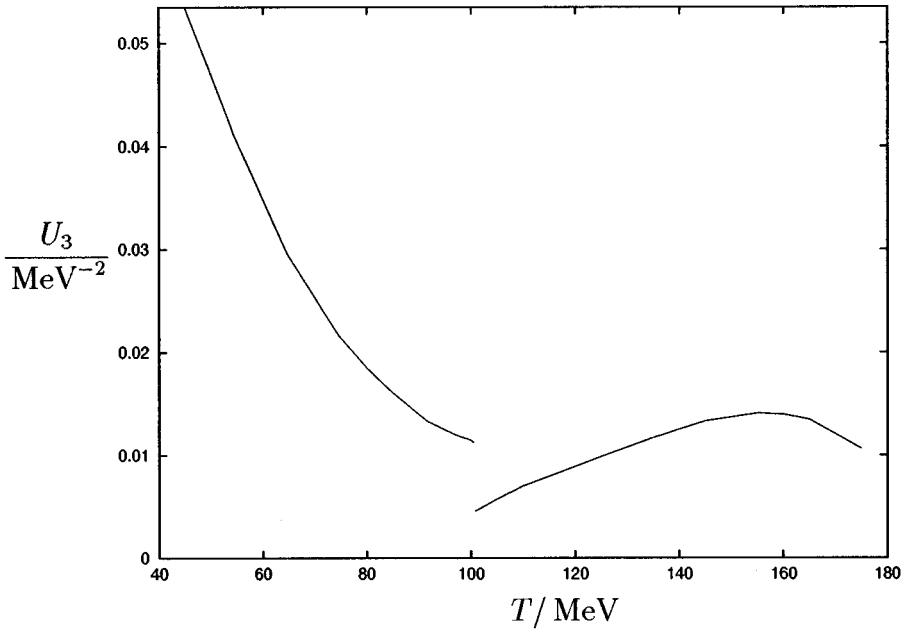

FIG. 9. The plot shows the renormalized Φ^6 scalar self coupling U_3 as a function of temperature T in the chiral limit.

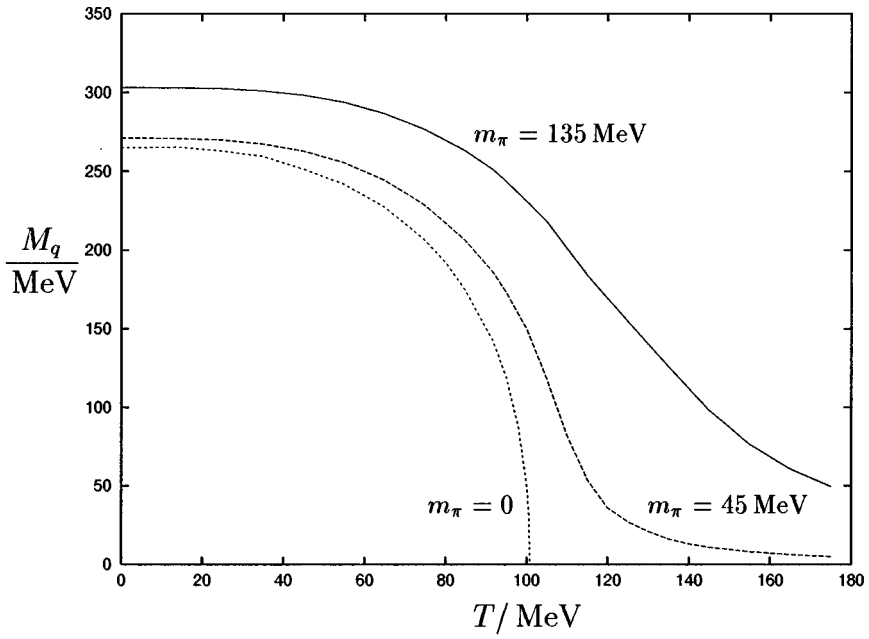

FIG. 10. The plot shows the constituent quark mass M_q as a function of T for three different values of the average light current quark mass $\hat{m}$. The solid line corresponds to the realistic value $\hat{m}=\hat{m}_{\text{phys}}$ whereas the dotted line represents the situation without explicit chiral symmetry breaking, i.e., $\hat{m}=0$. The intermediate, dashed line assumes $\hat{m}=\hat{m}_{\text{phys}}/10$.

ues of T. The curves cover a temperature range $T=(5-175)$ MeV. The first one to the left corresponds to $T=175$ MeV and neighboring curves differ in temperature by $\Delta T=10$ MeV. One observes only a weak dependence of $\partial U(T)/\partial\phi_R$ on the temperature for $T\lesssim 60$ MeV. Evaluated for $\phi_R=\sigma_0$ this function connects the renormalized field expectation value with $m_\pi(T)$, the source J and the mesonic wave function renormalization $Z_\Phi(T)$ according to

$$\frac{\partial U(T)}{\partial\phi_R}(\phi_R=\sigma_0)=\frac{2J}{Z_\Phi^{1/2}(T)}=4\sigma_0(T)m_\pi^2(T). \quad (4.2)$$

We close this section with a short assessment of the validity of our effective quark meson model as an effective description of two flavor QCD at non-vanishing temperature. The identification of qualitatively different scale intervals which appear in the context of chiral symmetry breaking, as presented in Sec. II A for the zero temperature case, can be generalized to $T\neq 0$: For scales below k_Φ there exists a hybrid description in terms of quarks and mesons. For $k_{\chi SB}\leqslant k\lesssim 600$ MeV chiral symmetry remains unbroken where the symmetry breaking scale $k_{\chi SB}(T)$ decreases with increasing temperature. Also the constituent quark mass decreases

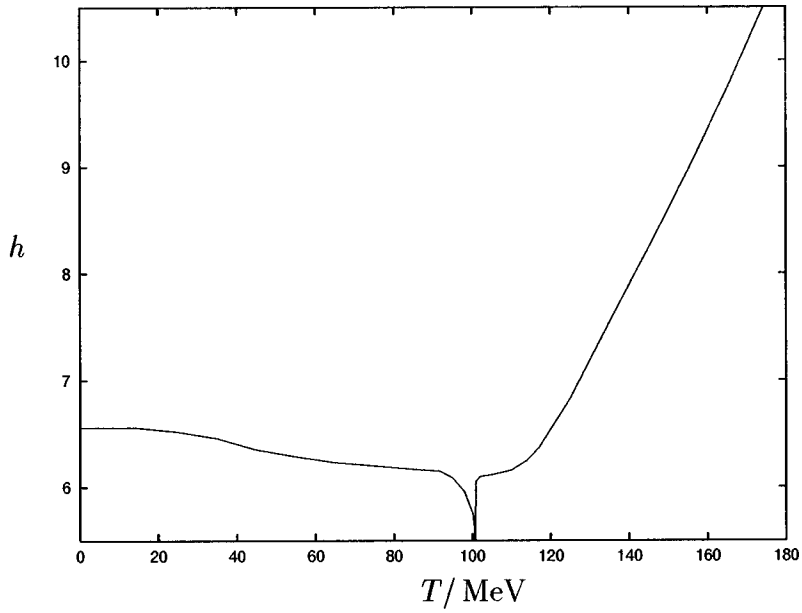

FIG. 11. The plot shows the Yukawa coupling, h, as a function of temperature T in the chiral limit.

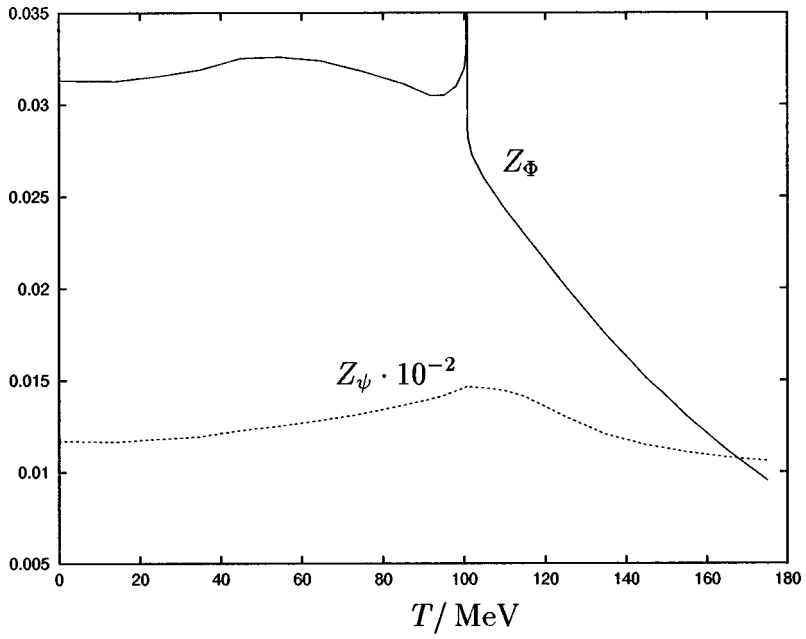

FIG. 12. The plot shows the scalar (solid line) and quark (dashed line) wave function renormalization constants, $Z_\Phi(T)$ and $Z_\psi(T) \times 10^{-2}$, respectively, as functions of temperature T for $\hat{m}=0$.

with T (cf. Fig. 10). The running Yukawa coupling depends only mildly on temperature for $T \lesssim 120$ MeV (see Fig. 11). (Only near the critical temperature and for $\hat{m}=0$ the running is extended because of massless pion fluctuations.) On the other hand, for $k \lesssim 4T$ the effective three-dimensional gauge coupling increases faster than at $T=0$ leading to an increase of $\Lambda_{\mathrm{QCD}}(T)$ with T [18]. As k gets closer to the scale $\Lambda_{\mathrm{QCD}}(T)$ it is no longer justified to neglect in the quark sector confinement effects which go beyond the dynamics of our present quark meson model. Here it is important to note that the quarks remain quantitatively relevant for the evolution of the meson degrees of freedom only for scales $k \gtrsim T/0.6$ (cf. Fig. 5, Sec. III). In the limit $k \ll T/0.6$ all fermionic Matsubara modes decouple from the evolution of the meson potential according to the temperature dependent version of Eq. (2.11). Possible sizeable confinement corrections

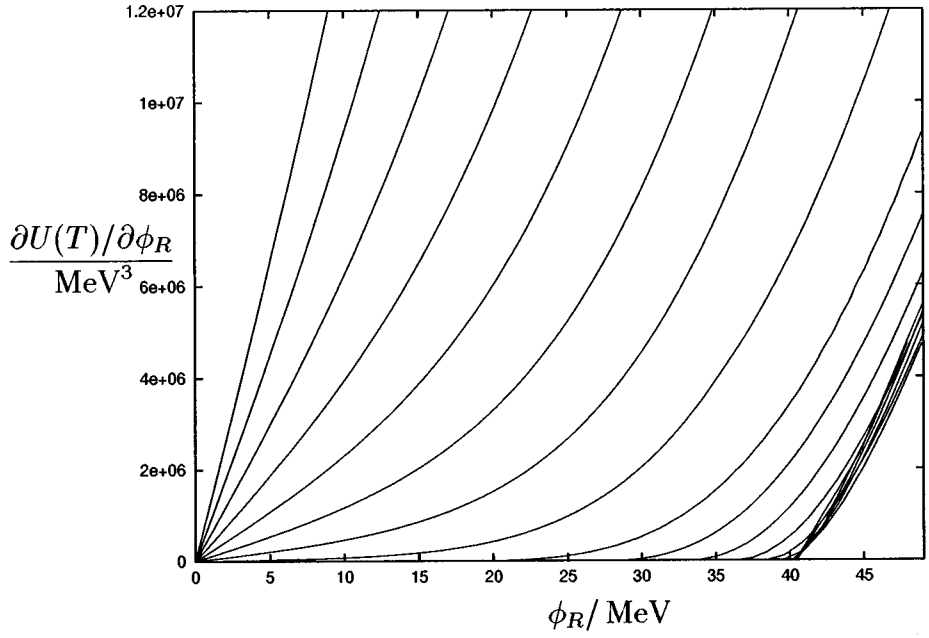

FIG. 13. The plot shows the derivative of the meson potential $U(T)$ with respect to the renormalized field $\phi_R=(Z_\Phi \rho/2)^{1/2}$ for different values of T. The first curve on the left corresponds to $T=175$ MeV. The successive curves to the right differ in temperature by $\Delta T=10$ MeV down to $T=5$ MeV.

TABLE III. The table shows the critical exponents corresponding to the three-dimensional $O(4)$-Heisenberg model. Our results are denoted by ''average action'' whereas ''FD'' labels the exponents obtained from the perturbation series at fixed dimension to seven loops [51]. The bottom line contains lattice Monte Carlo results [50].

	ν	γ	δ	β	η
Average action	0.787	1.548	4.80	0.407	0.0344
FD	0.73(2)	1.44(4)	4.82(5)	0.38(1)	0.03(1)
MC	0.7479(90)	1.477(18)	4.851(22)	0.3836(46)	0.0254(38)

to the meson physics may occur if $\Lambda_{\mathrm{QCD}}(T)$ becomes larger than the maximum of $M_q(T)$ and $T/0.6$. From Fig. 10 we infer that this is particularly dangerous for small $\hat{m}$ in a temperature interval around T_c. Nevertheless, the situation is not dramatically different from the zero temperature case since only a relatively small range of k is concerned. We do not expect that the neglected QCD non-localities lead to qualitative changes. Quantitative modifications, especially for small $\hat{m}$ and $|T-T_c|$ remain possible. This would only effect the non-universal amplitudes (see Sec. V). The size of these corrections depends on the strength of (non-local) deviations of the quark propagator and the Yukawa coupling from the values computed in the quark meson model.

V. UNIVERSAL CRITICAL BEHAVIOR

In this section we study the linear quark meson model in the vicinity of the critical temperature T_c close to the chiral limit $\hat{m}=0$. In this region we find that the sigma mass m_σ^{-1} is much larger than the inverse temperature T^{-1}, and one observes an effectively three-dimensional behavior of the high temperature quantum field theory. We also note that the fermions are no longer present in the dimensionally reduced system as has been discussed in Sec. III. We therefore have to deal with a purely bosonic $O(4)$-symmetric linear sigma model. At the phase transition the correlation length becomes infinite and the effective three-dimensional theory is dominated by classical statistical fluctuations. In particular, the critical exponents which describe the singular behavior of various quantities near the second order phase transition are those of the corresponding classical system.

Many properties of this system are universal, i.e. they only depend on its symmetry $[O(4)]$, the dimensionality of space (three) and its degrees of freedom (four real scalar components). Universality means that the long-range properties of the system do not depend on the details of the specific model like its short distance interactions. Nevertheless, important properties as the value of the critical temperature are non-universal. We emphasize that although we have to deal with an effectively three-dimensional bosonic theory, the non-universal properties of the system crucially depend on the details of the four-dimensional theory and, in particular, on the fermions.

Our aim is a computation of the critical equation of state which relates for arbitrary T near T_c the derivative of the free energy or effective potential U to the average current quark mass $\hat{m}$. The equation of state then permits to study the temperature and quark mass dependence of properties of the chiral phase transition.

At the critical temperature and in the chiral limit there is no scale present in the theory. In the vicinity of T_c and for small enough $\hat{m}$ one therefore expects a scaling behavior of the effective average potential u_k [45] and accordingly a universal scaling form of the equation of state. There are only two independent scales close to the transition point which can be related to the deviation from the critical temperature, $T-T_c$, and to the explicit symmetry breaking through the quark mass $\hat{m}$. As a consequence, the properly rescaled potential can only depend on one scaling variable. A possible choice for the parametrization of the rescaled ''unrenormalized'' potential is the use of the Widom scaling variable [46]

$$x=\frac{(T-T_c)/T_c}{(2\bar{\sigma}_0/T_c)^{1/\beta}}. \tag{5.1}$$

Here β is the critical exponent of the order parameter $\bar{\sigma}_0$ in the chiral limit $\hat{m}=0$ [see Eq. (5.5)]. With $U'(\rho=2\bar{\sigma}_0^2)=J/(2\bar{\sigma}_0)$ the Widom scaling form of the equation of state reads [46]

$$\frac{J}{T_c^3}=\left(\frac{2\bar{\sigma}_0}{T_c}\right)^{\delta} f(x) \tag{5.2}$$

where the exponent δ is related to the behavior of the order parameter according to Eq. (5.7). The equation of state (5.2) is written for convenience directly in terms of four-dimensional quantities. They are related to the corresponding effective variables of the three-dimensional theory by appropriate powers of T_c. The source J is determined by the average current quark mass $\hat{m}$ as $J=2\bar{m}_{k_\Phi}^2\hat{m}$. The mass term at the compositeness scale, $\bar{m}_{k_\Phi}^2$, also relates the chiral condensate to the order parameter according to $\langle\bar{\psi}\psi\rangle=-2\bar{m}_{k_\Phi}^2(\bar{\sigma}_0-\hat{m})$. The critical temperature of the linear quark meson model was found in Sec. IV to be $T_c=100.7$ MeV.

The scaling function f is universal up to the model specific normalization of x and itself. Accordingly, all models in the same universality class can be related by a rescaling of $\bar{\sigma}_0$ and $T-T_c$. The non-universal normalizations for the quark meson model discussed here are defined according to

$$f(0)=D, \quad f(-B^{-1/\beta})=0. \tag{5.3}$$

We find $D=1.82\times10^{-4}$, $B=7.41$ and our result for β is given in Table III. Apart from the immediate vicinity of the

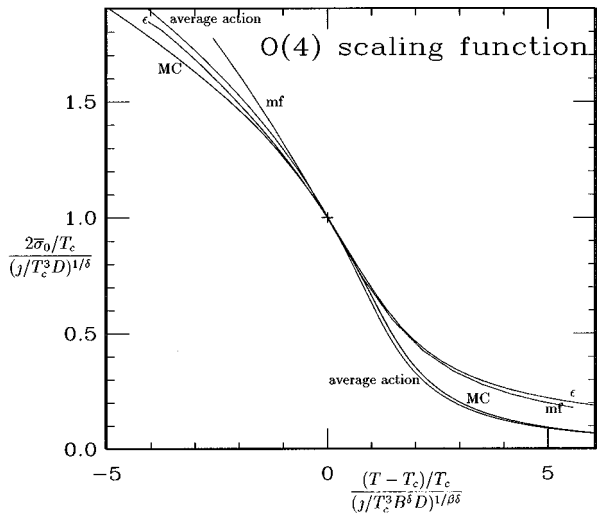

FIG. 14. The figure shows a comparison of our results, denoted by ''average action,'' with results of other methods for the scaling function of the three-dimensional $O(4)$ Heisenberg model. We have labeled the axes for convenience in terms of the expectation value $\bar{\sigma}_0$ and the source J of the corresponding four-dimensional theory. The constants B and D specify the non-universal amplitudes of the model [cf. Eq. (5.3)]. The curve labeled by ''MC'' represents a fit to lattice Monte Carlo data. The second order epsilon expansion [49] and mean field results are denoted by ''ϵ'' and ''mf,'' respectively. Apart from our results the curves are taken from Ref. [48].

zero of $f(x)$ we find the following two parameter fit (cf. Ref. [47]) for the scaling function

$$f_{\rm fit}(x) = 1.816\times 10^{-4}(1+136.1x)^2(1+160.9\theta x)^{\Delta} \times (1+160.9(0.9446\theta^{\Delta})^{-1/(\gamma-2-\Delta)}x)^{\gamma-2-\Delta} \tag{5.4}$$

to reproduce the numerical results for f and df/dx at the 1–2 % level with $\theta=0.625$ (0.656), $\Delta=-0.490$ (-0.550) for $x>0$ ($x<0$) and γ as given in Table III. The universal properties of the scaling function can be compared with results obtained by other methods for the three-dimensional $O(4)$ Heisenberg model. In Fig. 14 we display our results along with those obtained from lattice Monte Carlo simulation [48], second order epsilon expansion [49] and mean field theory. We observe a good agreement of average action, lattice and epsilon expansion results within a few percent for $T<T_c$. Above T_c the average action and the lattice curve go quite close to each other with a substantial deviation from the epsilon expansion and mean field scaling function.[12]

Before we use the scaling function $f(x)$ to discuss the general temperature and quark mass dependent case, we consider the limits $T=T_c$ and $\hat{m}=0$, respectively. In these limits the behavior of the various quantities is determined solely by critical amplitudes and exponents. In the spontaneously broken phase ($T<T_c$) and in the chiral limit we observe that the renormalized and unrenormalized order parameters scale according to

$$\frac{2\sigma_0(T)}{T_c} = (2E)^{1/2}\left(\frac{T_c-T}{T_c}\right)^{\nu/2},$$
$$\frac{2\bar{\sigma}_0(T)}{T_c} = B\left(\frac{T_c-T}{T_c}\right)^{\beta}, \tag{5.5}$$

respectively, with $E=0.814$ and the value of B given above. In the symmetric phase the renormalized mass $m=m_\pi=m_\sigma$ and the unrenormalized mass $\bar{m}=Z_\Phi^{1/2}m$ behave as

$$\frac{m(T)}{T_c} = (\xi^+)^{-1}\left(\frac{T-T_c}{T_c}\right)^{\nu},$$
$$\frac{\bar{m}(T)}{T_c} = (C^+)^{-1/2}\left(\frac{T-T_c}{T_c}\right)^{\gamma/2}, \tag{5.6}$$

where $\xi^+=0.270$, $C^+=2.79$. For $T=T_c$ and non-vanishing current quark mass we have

$$\frac{2\bar{\sigma}_0}{T_c} = D^{-1/\delta}\left(\frac{J}{T_c^3}\right)^{1/\delta} \tag{5.7}$$

with the value of D given above.

Though the five amplitudes E, B, ξ^+, C^+ and D are not universal there are ratios of amplitudes which are invariant under a rescaling of $\bar{\sigma}_0$ and $T-T_c$. Our results for the universal amplitude ratios are

$$R_\chi = C^+DB^{\delta-1} = 1.02,$$
$$\tilde{R}_\xi = (\xi^+)^{\beta/\nu}D^{1/(\delta+1)}B = 0.852,$$
$$\xi^+E = 0.220. \tag{5.8}$$

Those for the critical exponents are given in Table III. Here the value of η is obtained from the temperature dependent version of Eq. (2.16) (cf. Appendix C) at the critical temperature. For comparison, Table III also gives the results from the perturbation series at fixed dimension to seven loop order [51,52] as well as lattice Monte Carlo results [50] which have been used for the lattice form of the scaling function in Fig. 14.[13] There are only two independent amplitudes and critical exponents, respectively. They are related by the usual scaling relations of the three-dimensional scalar $O(N)$ model [52] which we have explicitly verified by the independent calculation of our exponents.

We turn to the discussion of the scaling behavior of the chiral condensate $\langle\bar{\psi}\psi\rangle$ for the general case of a temperature and quark mass dependence. In Fig. 1 in the Introduction we

[12]We note that the question of a better agreement of the curves for $T<T_c$ or $T>T_c$ depends on the chosen non-universal normalization conditions for x and f [cf. Eq. (5.3)].

[13]See also Ref. [53] and references therein for a recent calculation of critical exponents using similar methods as in this work. For high precision estimates of the critical exponents see also Refs. [54, 55].

have displayed our results for the scaling equation of state in terms of the chiral condensate[14]

$$\langle\bar{\psi}\psi\rangle = -\bar{m}_{k_\Phi}^2 T_c\left(\frac{J/T_c^3}{f(x)}\right)^{1/\delta} + J \tag{5.9}$$

as a function of $T/T_c = 1 + x(J/T_c^3 f(x))^{1/\beta\delta}$ for different quark masses or, equivalently, different values of J. The curves shown in Fig. 1 correspond to quark masses $\hat{m}=0$, $\hat{m}=\hat{m}_{\rm phys}/10$, $\hat{m}=\hat{m}_{\rm phys}$ and $\hat{m}=3.5\hat{m}_{\rm phys}$ or, equivalently, to zero temperature pion masses $m_\pi=0$, $m_\pi=45$ MeV, $m_\pi=135$ MeV and $m_\pi=230$ MeV, respectively (cf. Fig. 4). One observes that the second order phase transition with a vanishing order parameter at T_c for $\hat{m}=0$ is turned into a smooth crossover in the presence of non-zero quark masses.

The scaling form (5.9) for the chiral condensate is exact only in the limit $T\to T_c$, $J\to 0$. It is interesting to find the range of temperatures and quark masses for which $\langle\bar{\psi}\psi\rangle$ approximately shows the scaling behavior (5.9). This can be inferred from a comparison (see Fig. 1) with our full non-universal solution for the T and J dependence of $\langle\bar{\psi}\psi\rangle$ as described in Sec. IV. For $m_\pi=0$ one observes approximate scaling behavior for temperatures $T\gtrsim 90$ MeV. This situation persists up to a pion mass of $m_\pi=45$ MeV. Even for the realistic case, $m_\pi=135$ MeV, and to a somewhat lesser extent for $m_\pi=230$ MeV the scaling curve reasonably reflects the physical behavior for $T\gtrsim T_c$. For temperatures below T_c, however, the zero temperature mass scales become important and the scaling arguments leading to universality break down.

The above comparison may help to shed some light on the use of universality arguments away from the critical temperature and the chiral limit. One observes that for temperatures above T_c the scaling assumption leads to quantitatively reasonable results even for a pion mass almost twice as large as the physical value. This in turn has been used for two flavor lattice QCD as theoretical input to guide extrapolation of results to light current quark masses. From simulations based on a range of pion masses $0.3\lesssim m_\pi/m_\rho\lesssim 0.7$ and temperatures $0<T\lesssim 250$ MeV a ''pseudocritical temperature'' of approximately 140 MeV with a weak quark mass dependence is reported [56]. Here the ''pseudocritical temperature'' T_{pc} is defined as the inflection point of $\langle\bar{\psi}\psi\rangle$ as a function of temperature. The values of the lattice action parameters used in [56] with $N_t=6$ were $a\hat{m}=0.0125$, $6/g^2=5.415$ and $a\hat{m}=0.025$, $6/g^2=5.445$. For comparison with lattice data we have displayed in Fig. 1 the temperature dependence of the chiral condensate for a pion mass $m_\pi=230$ MeV. From the free energy of the linear quark meson model we obtain in this case a pseudocritical temperature of about 150 MeV in reasonable agreement with the results of Ref. [56]. In contrast, for the critical temperature in the chiral limit we obtain $T_c=100.7$ MeV. This value is considerably smaller than the lattice results of about (140–150) MeV obtained by extrapolating to zero quark mass in Ref. [56]. We point out that for pion masses as large as 230 MeV the condensate $\langle\bar{\psi}\psi\rangle(T)$ is almost linear around the inflection point for quite a large range of temperature. This makes a precise determination of T_c somewhat difficult. Furthermore, Fig. 1 shows that the scaling form of $\langle\bar{\psi}\psi\rangle(T)$ underestimates the slope of the physical curve. Used as a fit with T_c as a parameter this can lead to an overestimate of the pseudocritical temperature in the chiral limit. We also mention here the results of Ref. [57]. There two values of the pseudocritical temperature, $T_{pc}=150(9)$ MeV and $T_{pc}=140(8)$, corresponding to $a\hat{m}=0.0125$, $6/g^2=5.54(2)$ and $a\hat{m}=0.00625$, $6/g^2=5.49(2)$, respectively (both for $N_t=8$), were computed. These values show a somewhat stronger quark mass dependence of T_{pc} and were used for a linear extrapolation to the chiral limit yielding $T_c=128(9)$ MeV.

The linear quark meson model exhibits a second order phase transition for two quark flavors in the chiral limit. As a consequence the model predicts a scaling behavior near the critical temperature and the chiral limit which can, in principle, be tested in lattice simulations. For the quark masses used in the present lattice studies the order and universality class of the transition in two flavor QCD remain a partially open question. Though there are results from the lattice giving support for critical scaling [58,59] there are also recent simulations with two flavors that reveal significant finite size effects and problems with $O(4)$ scaling [60,61].

VI. ADDITIONAL DEGREES OF FREEDOM

So far we have investigated the chiral phase transition of QCD as described by the linear $O(4)$ model containing the three pions and the sigma resonance as well as the up and down quarks as degrees of freedom. Of course, it is clear that the spectrum of QCD is much richer than the states incorporated in our model. It is therefore important to ask to what extent the neglected degrees of freedom like the strange quark, strange (pseudo)scalar mesons, (axial)vector mesons, baryons, etc., might be important for the chiral dynamics of QCD. Before doing so it is perhaps instructive to first look into the opposite direction and investigate the difference between the linear quark meson model described here and chiral perturbation theory based on the non-linear sigma model [34]. In some sense, chiral perturbation theory is the minimal model of chiral symmetry breaking containing only the Goldstone degrees of freedom. By construction it is therefore only valid in the spontaneously broken phase and cannot be expected to yield realistic results for temperatures close to T_c or for the symmetric phase. However, for small temperatures (and momentum scales) the non-linear model is expected to describe the low-energy and low-temperature limit of QCD reliably as an expansion in powers of the light quark masses. For vanishing temperature it has been demonstrated recently [36,37] that the results of chiral perturbation theory can be reproduced within the linear meson model once certain higher dimensional operators in its effective action are taken into account for the three flavor case. Moreover, some of the parameters of chiral perturbation theory $(L_4,\ldots,L_8)$ can be

[14]In the literature also a different definition of the chiral condensate is used, corresponding to $\langle\bar{\psi}\psi\rangle = -\bar{m}_{k_\Phi}^2 T_c[J/(T_c^3 f(x))]^{1/\delta}$.

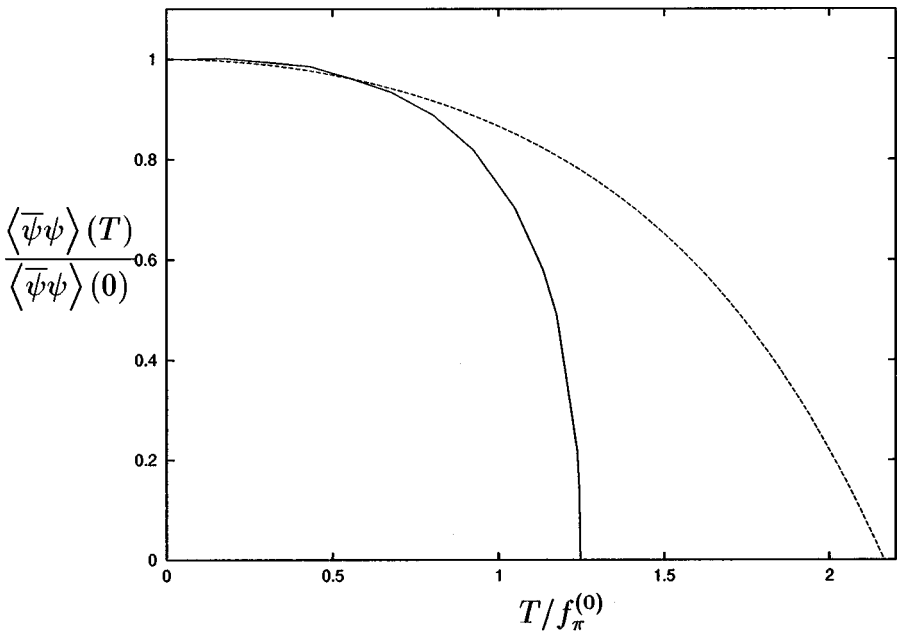

FIG. 15. The plot displays the chiral condensate $\langle\bar{\psi}\psi\rangle$ as a function of $T/f_\pi^{(0)}$. The solid line corresponds to our results for vanishing average current quark mass $\hat{m}=0$ whereas the dashed line shows the corresponding three-loop chiral perturbation theory result for $\Gamma_1 = 470$ MeV.

expressed and therefore also numerically computed in terms of those of the linear model. For non-vanishing temperature one expects agreement only for low T whereas deviations from chiral perturbation theory should become large close to T_c. Yet, even for $T \ll T_c$ small quantitative deviations should exist because of the contributions of (constituent) quark and sigma meson fluctuations in the linear model which are not taken into account in chiral perturbation theory.

From [62] we infer the three-loop result for the temperature dependence of the chiral condensate in the chiral limit for N light flavors

$$\langle\bar{\psi}\psi\rangle(T)_{\chi PT}=\langle\bar{\psi}\psi\rangle_{\chi PT}(0)\left\{1-\frac{N^2-1}{N}\frac{T^2}{12F_0^2}-\frac{N^2-1}{2N^2}\left(\frac{T^2}{12F_0^2}\right)^2+N(N^2-1)\left(\frac{T^2}{12F_0^2}\right)^3\ln\frac{T}{\Gamma_1}\right\}+\mathcal{O}(T^8). \tag{6.1}$$

The scale Γ_1 can be determined from the D-wave isospin zero $\pi\pi$ scattering length and is given by $\Gamma_1=(470 \pm 100)$ MeV. The constant F_0 is (in the chiral limit) identical to the pion decay constant $F_0=f_\pi^{(0)}=80.8$ MeV. In Fig. 15 we have plotted the chiral condensate as a function of T/F_0 for both, chiral perturbation theory according to Eq. (6.1) and for the linear quark meson model. As expected the agreement for small T is very good. Nevertheless, the anticipated small numerical deviations present even for $T \ll T_c$ due to quark and sigma meson loop contributions are manifest. For larger values of T, say for $T \gtrsim 0.8 f_\pi^{(0)}$ the deviations become significant because of the intrinsic inability of chiral perturbation theory to correctly reproduce the critical behavior of the system near its second order phase transition.

Within the language of chiral perturbation theory the neglected effects of thermal quark fluctuations may be described by an effective temperature dependence of the parameter $F_0(T)$. We notice that the temperature at which these corrections become important equals approximately one third of the constituent quark mass $M_q(T)$ or the sigma mass $m_\sigma(T)$, respectively, in perfect agreement with Fig. 5. As suggested by this figure the onset of the effects from thermal fluctuations of heavy particles with a T-dependent mass $m_H(T)$ is rather sudden for $T \gtrsim m_H(T)/3$. These considerations also apply to our two flavor quark meson model. Within full QCD we expect temperature dependent initial values at k_Φ.

The dominant contribution to the temperature dependence of the initial values presumably arises from the influence of the mesons containing strange quarks as well as the strange quark itself. Here the quantity $\bar{m}^2_{k_\Phi}$ seems to be the most important one. [The temperature dependence of higher couplings like $\lambda(T)$ is not very relevant if the IR attractive behavior remains valid, i.e. if Z_{Φ,k_Φ} remains small for the range of temperatures considered. We neglect a possible T dependence of the current quark mass $\hat{m}$.] In particular, for three flavors the potential U_{k_Φ} contains a term

$$-\frac{1}{2}\,\bar{\nu}_{k_\Phi}(\det\Phi+\det\Phi^\dagger)=-\bar{\nu}_{k_\Phi}\varphi_s\Phi_{uu}\Phi_{dd}+\cdots \tag{6.2}$$

which reflects the axial $U_A(1)$ anomaly. It yields a contribution to the effective mass term proportional to the expectation value $\langle\Phi_{ss}\rangle\equiv\varphi_s$, i.e.

$$\Delta\bar{m}^2_{k_\Phi} = -\frac{1}{2}\,\bar{\nu}_{k_\Phi}\varphi_s\,. \tag{6.3}$$

Both, $\bar{\nu}_{k_\Phi}$ and φ_s, depend on T. We expect these corrections to become relevant only for temperatures exceeding $m_K(T)/3$ or $M_s(T)/3$. We note that the temperature dependent kaon and strange quark masses, $m_K(T)$ and $M_s(T)$, respectively, may be somewhat different from their zero temperature values but we do not expect them to be much smaller. A typical value for these scales is around 500 MeV. Correspondingly, the thermal fluctuations neglected in our model should become important for $T \gtrsim 170$ MeV. It is even conceivable that a discontinuity appears in $\varphi_s(T)$ for sufficiently high T (say $T \simeq 170$ MeV). This would be reflected by a discontinuity in the initial values of the $O(4)$ model leading to a first order transition within this model. Obviously, these questions should be addressed in the framework of the three flavor $SU_L(3)\times SU_R(3)$ quark meson model. Work in this direction is in progress.

We note that the temperature dependence of $\bar{\nu}(T)\varphi_s(T)$ is closely related to the question of an effective high temperature restoration of the axial $U_A(1)$ symmetry [3,8]. The η' mass term is directly proportional to this combination, $m^2_{\eta'}(T) - m^2_\pi(T) \simeq \frac{3}{2}\bar{\nu}(T)\varphi_s(T)$ [35]. Approximate $U_A(1)$ restoration would occur if $\varphi_s(T)$ or $\bar{\nu}(T)$ would decrease sizeably for large T. For realistic QCD this question should be addressed by a three flavor study. Within two flavor QCD the combination $\bar{\nu}_k\varphi_s$ is replaced by an effective anomalous mass term $\bar{\nu}^{(2)}_k$. The temperature dependence of $\bar{\nu}^{(2)}(T)$ could be studied by introducing quarks and the axial anomaly in the two flavor matrix model of Ref. [39]. We add that this question has also been studied within full two flavor QCD in lattice simulations [60,63,64]. So far there does not seem to be much evidence for a restoration of the $U_A(1)$ symmetry near T_c but no final conclusion can be drawn yet.

To summarize, we have found that the effective two flavor quark meson model presumably gives a good description of the temperature effects in two flavor QCD for a temperature range $T \lesssim 170$ MeV. Its reliability should be best for low temperature where our results agree with chiral perturbation theory. However, the range of validity is considerably extended as compared to chiral perturbation theory and includes, in particular, the critical temperature of the second order phase transition in the chiral limit. We have explicitly connected the universal critical behavior for small $|T-T_c|$ and small current quark masses with the renormalized couplings at $T=0$ and realistic quark masses. The main quantitative uncertainties from neglected fluctuations presumably concern the values of $f^{(0)}_\pi$ and T_c which, in turn, influence the non-universal amplitudes B and D in the critical region. We believe that our overall picture is rather solid. Where applicable our results compare well with numerical simulations of full two flavor QCD.

ACKNOWLEDGMENTS

This work was supported by the Deutsche Forschungsgemeinschaft. We thank K. Rajagopal for very useful comments.

APPENDIX A: THE QUARK MASS TERM

In this appendix we determine the source $J = \mathrm{diag}(j_u, j_d, ...)$ as a function of the average current quark mass $\hat{m}$. In this context it is important to note that the source J does not depend on the IR cutoff scale k. Since J is determined by the properties of the quark meson model at the compositeness scale k_Φ and also enters directly the value of the pion mass, which is determined at $k=0$, this relation provides a bridge between the short and long distance properties of the quark meson model. This will allow us to compute the chiral condensate $\langle\bar{\psi}\psi\rangle$ or the parameter B_0 of chiral perturbation theory [34]. (We expect, however, sizeable corrections when going from two to three flavors. They arise because of the relevance of strange quark physics at scales near k_Φ.) In a more general context we need the proportionality coefficient a_q between the source J_q and the current quark mass m_q, $q=u,d,\ldots$, taken at the renormalization scale[15] $\mu = k_\Phi$:

$$J_q = \frac{Z_{\psi,k_\Phi}}{\bar{h}_{k_\Phi}}\,a_q m_q\,. \tag{A1}$$

For a computation of the coefficient a_q we need to look into the details of the introduction of composite meson fields in QCD [26,28]. Let us assume that at the scale k_Φ a part of the QCD average action for quarks $\Gamma_{k_\Phi}[\psi]$ factorizes in the quark bilinear

$$\chi_{ab}(q) = -\int \frac{d^4p}{(2\pi)^4}\,\tilde{g}(p,q)\,\bar{\psi}_{Lb}(p)\,\psi_{Ra}(p+q) \tag{A2}$$

such that

$$\Gamma_{k_\Phi}[\psi] = -F_{k_\Phi}[\chi] + \Gamma'_{k_\Phi}[\psi]. \tag{A3}$$

We can then introduce meson fields by inserting the identity

$$N\int D\Phi\ \exp(-F_{k_\Phi}[\chi+\Phi]) = 1 \tag{A4}$$

into the path integral which formally defines $\Gamma_{k_\Phi}[\psi]$. (Here N is a field independent normalization factor.) This effectively replaces in Eq. (A3) the term $-F_{k_\Phi}[\chi]$ by[16]

[15] We will occasionally use the notation $\hat{m}(\mu)$, $m_q(\mu)$ or $\langle\bar{\psi}\psi\rangle(\mu) \equiv \langle\bar{\psi}\psi\rangle_{k=0}(\mu)$ [not to be confused with $\langle\bar{\psi}\psi\rangle_k \equiv \langle\bar{\psi}\psi\rangle_k(\mu=k_\Phi)$] in order to indicate the renormalization scale μ. If no argument is given $\mu = k_\Phi$ is assumed.

[16] The summation over internal indices as well as the integration over momenta has been suppressed. For complex $\chi_{ab}(q)$ similar terms have to be supplemented in the expansion. See Refs. [26,28] for a more detailed description. In our Euclidean conventions one has $\chi^\dagger_{ab} \sim +\tilde{g}^*\bar{\psi}_{Rb}\psi_{La}$.

$$-F_{k_\Phi}[\chi]+F_{k_\Phi}[\chi+\Phi] = \frac{\partial F_{k_\Phi}[\chi]}{\partial\chi_{ab}(q)}\Phi_{ab}(q)+\frac{1}{2}\frac{\partial^2 F_{k_\Phi}[\chi]}{\partial\chi_{ab}(q)\partial\chi_{cd}(q')} \times\Phi_{ab}(q)\Phi_{cd}(q')+\cdots . \tag{A5}$$

The original multi-quark interaction $-F_{k_\Phi}[\chi]$ is canceled by the lowest order term in the Taylor expansion in Φ. Instead, we have substituted mesonic self-interactions $F_{k_\Phi}[\Phi]$ and interactions between mesons and quarks corresponding to the terms in the expansion which contain powers of χ and Φ. In particular, we may specialize to the case where the derivative terms in F_{k_Φ} are small and consider a local form $F_{k_\Phi}=\int d^4x f_{k_\Phi}(\chi)$. A quark mass term is linear in χ and translates into a source term for Φ:

$$-\frac{Z_{\psi,k_\Phi}}{\tilde g}\,\mathrm{Tr}(\chi^\dagger m+m^\dagger\chi)\to-\frac{Z_{\psi,k_\Phi}}{\tilde g}\,\mathrm{Tr}(\Phi^\dagger m+m^\dagger\Phi) = -\frac{1}{2}\,\mathrm{Tr}(\Phi^\dagger J+J^\dagger\Phi) \tag{A6}$$

where $m=\mathrm{diag}(m_u,m_d,...)$. A factorizing four fermion interaction yields

$$\bar m^2_{k_\Phi}\ \mathrm{Tr}\ \chi^\dagger\chi\to\bar m^2_{k_\Phi}\ \mathrm{Tr}\ \Phi^\dagger\Phi+\bar m^2_{k_\Phi}\ \mathrm{Tr}(\Phi^\dagger\chi+\chi^\dagger\Phi). \tag{A7}$$

The second term corresponds to the Yukawa interaction with $\bar h_{k_\Phi}=\bar m^2_{k_\Phi}\tilde g$. We can therefore extract a_q from Eq. (A6) as

$$a_q=2\bar m^2_{k_\Phi}. \tag{A8}$$

We note that only the terms linear and quadratic in χ influence the value of a_q. We could either restrict the composite fields from the beginning to the ones contained in the $O(4)$-symmetric linear σ-model or work with all the fields contained in a complex 2×2 matrix Φ. In the latter case the anomaly term would contribute to both the masses and the Yukawa coupling. The net result is the same with $\bar m^2_{k_\Phi}$ denoting the relevant mass term for the $O(4)$ vector. For our conventions with $\bar h_{k_\Phi}=1$ we have to normalize with $\tilde g=\bar m^{-2}_{k_\Phi}$. Finally an eight fermion interaction becomes

$$\frac{1}{2}\,\bar\lambda_{k_\Phi}(\mathrm{Tr}\ \chi^\dagger\chi)^2\to\frac{1}{2}\,\bar\lambda_{k_\Phi}(\mathrm{Tr}\ \Phi^\dagger\Phi)^2 +\bar\lambda_{k_\Phi}\ \mathrm{Tr}\ \Phi^\dagger\Phi\ \mathrm{Tr}(\chi^\dagger\Phi+\Phi^\dagger\chi)+\cdots . \tag{A9}$$

We see here the appearance of terms quadratic in the quarks involving higher powers of Φ.

There is an alternative, equivalent way of understanding the relation between J and m_q: The quark masses in the picture with mesons must be equal at the scale k_Φ to the current quark mass $m_q(k_\Phi)$. Let us consider an $O(4)$-symmetric fermionic interaction $\bar m^2_{k_\Phi}\ \mathrm{Tr}\ \chi^\dagger\chi+\frac{1}{2}\bar\lambda_{k_\Phi}(\mathrm{Tr}\ \chi^\dagger\chi)^2$ which leads to a meson potential

$$U_{k_\Phi}=\bar m^2_{k_\Phi}\ \mathrm{Tr}\ \Phi^\dagger\Phi+\frac{1}{2}\,\bar\lambda_{k_\Phi}(\mathrm{Tr}\ \Phi^\dagger\Phi)^2. \tag{A10}$$

In the mesonic picture the quarks acquire masses through the Yukawa coupling to Φ

$$M_k=\frac{\bar h_k}{Z_{\psi,k}}\left(1+\frac{\bar\lambda_k}{\bar m^2_k}\,\mathrm{Tr}\langle\Phi^\dagger\rangle_k\langle\Phi\rangle_k\right)\langle\Phi\rangle_k \tag{A11}$$

where the second term arises from the higher order coupling in Eq. (A9). Here $\langle\Phi\rangle_k=\mathrm{diag}(\varphi_u,\varphi_d,...)$ is the expectation value at the coarse graining scale k in the presence of the source term and $M_k=\mathrm{diag}(M_u,M_d,...)$. It is sufficient to specify the dependence of U_{k_Φ} on real diagonal fields Φ_{qq}. Then the φ_q are determined from the condition

$$\frac{\partial U_{k_\Phi}}{\partial\Phi_{qq}}(\varphi_q)=2\left(\bar m^2_{k_\Phi}+\bar\lambda_{k_\Phi}\sum_{q'}\ \varphi^2_{q'}\right)\varphi_q=J_q. \tag{A12}$$

Identifying $M_{k=k_\Phi}$ in Eq. (A11) with $m(k_\Phi)$ one has

$$a_q\left(1+\frac{\bar\lambda_{k_\Phi}}{\bar m^2_{k_\Phi}}\sum_{q'}\ \varphi^2_{q'}\right)=\frac{J_q}{\varphi_q}=2\bar m^2_{k_\Phi}+2\bar\lambda_{k_\Phi}\sum_{q'}\ \varphi^2_{q'}, \tag{A13}$$

and we recover Eq. (A8) or, in our normalization with $Z_{\psi,k_\Phi}=1$, $\bar h_{k_\Phi}=1$,

$$J=2\bar m^2_{k_\Phi}\hat m. \tag{A14}$$

It is remarkable that higher order terms (e.g. $\sim\bar\lambda_{k_\Phi}$) do not influence the relation between J and $\hat m$. Only the quadratic term $\bar m^2_{k_\Phi}$ enters which is in our scenario the only relevant coupling. This feature is an important ingredient for the predictive power of the model as far as the absolute size of the current quark mass is concerned. An appearance of higher order couplings in a_q would make it very hard to compute this quantity. We emphasize that within our formalism there is no difference of principle between the current quark mass and the constituent quark mass. Whereas the current quark mass $m_q(k_\Phi)$ at the normalization scale $\mu=k_\Phi$ corresponds to $M_{q,k}$ at the compositeness scale k_Φ the constituent quark mass is $M_{q,k=0}$. As k is lowered from k_Φ to zero one observes that the quark mass increases, similarly to the running current quark mass. Once chiral symmetry breaking sets in at the scale $k_{\chi SB}$ there is a large increase in the quark masses, especially for M_u and M_d.

The formalism of composite fields also provides the link [26] to the chiral condensate $\langle\bar\psi\psi\rangle$ since the expectation value $\langle\Phi\rangle$ is related to the expectation value of a composite quark-antiquark operator. For $\bar\lambda=0$ one has [28]

$$\langle\Phi\rangle_k+\langle\Phi^\dagger\rangle_k=-\frac{1}{\bar{m}^2_{k_\Phi}}\langle\bar{\psi}\psi\rangle_k(k_\Phi)+m_q(k_\Phi)+m_q^\dagger(k_\Phi) \tag{A15}$$

with $\langle\bar{\psi}\psi\rangle_k(k_\Phi)$ a suitably regularized operator normalized at $\mu=k_\Phi$.

APPENDIX B: THRESHOLD FUNCTIONS

In this appendix we list the various definitions of dimensionless threshold functions appearing in the flow equations and the expressions for the anomalous dimensions for $T=0$. They involve the inverse scalar average propagator $P(q)$ defined in Eq. (1.4) and the corresponding fermionic function P_F which can be chosen as [27]

$$P_F(q)=P(q)\equiv q^2(1+r_F(q))^2. \tag{B1}$$

We abbreviate

$$x=q^2,\quad P(x)\equiv P(q),\dot{P}(x)\equiv\frac{\partial}{\partial x}P(x),\quad \frac{\hat{\partial}}{\partial t}\dot{P}\equiv\frac{\partial}{\partial x}\frac{\hat{\partial}}{\partial t}P, \tag{B2}$$

etc., and use the formal definition

$$\frac{\hat{\partial}}{\partial t}\equiv\frac{1}{Z_{\Phi,k}}\frac{\partial R_k}{\partial t}\frac{\partial}{\partial P}+\frac{2}{Z_{\psi,k}}\frac{P_F}{1+r_F}\frac{\partial[Z_{\psi,k}r_F]}{\partial t}\frac{\partial}{\partial P_F}. \tag{B3}$$

The bosonic threshold functions read

$$\begin{aligned}l_n^d(w;\eta_\Phi)&=l_n^d(w)-\eta_\Phi\hat{l}_n^d(w)\\&=\frac{n+\delta_{n,0}}{2}k^{2n-d}\int_0^\infty dx x^{d/2-1}\\&\quad\times\left(\frac{1}{Z_{\Phi,k}}\frac{\partial R_k}{\partial t}\right)(P+wk^2)^{-(n+1)}\end{aligned}$$

$$\begin{aligned}l^d_{n_1,n_2}(w_1,w_2;\eta_\Phi)&=l^d_{n_1,n_2}(w_1,w_2)-\eta_\Phi\hat{l}^d_{n_1,n_2}(w_1,w_2)\\&=-\frac{1}{2}k^{2(n_1+n_2)-d}\int_0^\infty dx x^{d/2-1}\frac{\hat{\partial}}{\partial t}\\&\quad\times\{(P+w_1k^2)^{-n_1}(P+w_2k^2)^{-n_2}\}\end{aligned} \tag{B4}$$

where $n,n_1,n_2\geqslant 0$ is assumed. For $n\neq 0$ the functions l_n^d may also be written as

$$\begin{aligned}l_n^d(w;\eta_\Phi)&=-\frac{1}{2}k^{2n-d}\int_0^\infty dx x^{d/2-1}\frac{\hat{\partial}}{\partial t}\\&\quad\times(P+wk^2)^{-n}.\end{aligned} \tag{B5}$$

The fermionic integrals $l_n^{(F)d}(w;\eta_\psi)=l_n^{(F)d}(w)-\eta_\psi\check{l}_n^{(F)d}(w)$ are defined analogously as

$$\begin{aligned}l_n^{(F)d}(w;\eta_\psi)&=(n+\delta_{n,0})k^{2n-d}\\&\quad\times\int_0^\infty dx x^{d/2-1}\frac{1}{Z_{\psi,k}}\frac{P_F}{1+r_F}\\&\quad\times\frac{\partial[Z_{\psi,k}r_F]}{\partial t}(P+wk^2)^{-(n+1)}.\end{aligned} \tag{B6}$$

Furthermore one has

$$\begin{aligned}l^{(FB)d}_{n_1,n_2}(w_1,w_2;\eta_\psi,\eta_\Phi)&=l^{(FB)d}_{n_1,n_2}(w_1,w_2)-\eta_\psi\check{l}^{(FB)d}_{n_1,n_2}(w_1,w_2)\\&\quad-\eta_\Phi\hat{l}^{(FB)d}_{n_1,n_2}(w_1,w_2)\\&=-\frac{1}{2}k^{2(n_1+n_2)-d}\int_0^\infty dx x^{d/2-1}\frac{\hat{\partial}}{\partial t}\\&\quad\times\left\{\frac{1}{[P_F(x)+k^2w_1]^{n_1}[P(x)+k^2w_2]^{n_2}}\right\}\end{aligned}$$

$$\begin{aligned}m^d_{n_1,n_2}(w_1,w_2;\eta_\Phi)&\equiv m^d_{n_1,n_2}(w_1,w_2)-\eta_\Phi\hat{m}^d_{n_1,n_2}(w_1,w_2)\\&=-\frac{1}{2}k^{2(n_1+n_2-1)-d}\int_0^\infty dx x^{d/2}\frac{\hat{\partial}}{\partial t}\\&\quad\times\left\{\frac{\dot{P}(x)}{[P(x)+k^2w_1]^{n_1}}\frac{\dot{P}(x)}{[P(x)+k^2w_2]^{n_2}}\right\}\end{aligned}$$

$$\begin{aligned}m_4^{(F)d}(w;\eta_\psi)&=m_4^{(F)d}(w)-\eta_\psi\check{m}_4^{(F)d}(w)\\&=-\frac{1}{2}k^{4-d}\int_0^\infty dx x^{d/2+1}\frac{\hat{\partial}}{\partial t}\\&\quad\times\left(\frac{\partial}{\partial x}\frac{1+r_F(x)}{P_F(x)+k^2w}\right)^2\end{aligned}$$

$$\begin{aligned}m^{(FB)d}_{n_1,n_2}(w_1,w_2;\eta_\psi,\eta_\Phi)&=m^{(FB)d}_{n_1,n_2}(w_1,w_2)-\eta_\psi\check{m}^{(FB)d}_{n_1,n_2}(w_1,w_2)\\&\quad-\eta_\Phi\hat{m}^{(FB)d}_{n_1,n_2}(w_1,w_2)\\&=-\frac{1}{2}k^{2(n_1+n_2-1)-d}\int_0^\infty dx x^{d/2}\frac{\hat{\partial}}{\partial t}\\&\quad\times\left\{\frac{1+r_F(x)}{[P_F(x)+k^2w_1]^{n_1}}\frac{\dot{P}(x)}{[P(x)+k^2w_2]^{n_2}}\right\}.\end{aligned} \tag{B7}$$

The dependence of the threshold functions on the anomalous dimensions arises from the t derivative acting on $Z_{\Phi,k}$ and $Z_{\psi,k}$ within R_k and $Z_{\psi,k}r_F$, respectively. We furthermore use the abbreviations

$$l_n^d(\eta_\Phi) \equiv l_n^d(0;\eta_\Phi),$$
$$l_n^{(F)d}(\eta_\psi) \equiv l_n^{(F)d}(0;\eta_\psi)$$
$$l_n^d(w) \equiv l_n^d(w;0),$$
$$l_n^d \equiv l_n^d(0;0) \tag{B8}$$

etc. and note that in four dimensions the integrals

$$l_2^4(0,0) = l_2^{(F)4}(0,0) = l_{1,1}^{(FB)4}(0,0)$$
$$= m_4^{(F)4}(0) = m_{1,2}^{(FB)4}(0,0) = 1 \tag{B9}$$

are independent of the particular choice of the infrared cutoff.

APPENDIX C: TEMPERATURE DEPENDENT THRESHOLD FUNCTIONS

Non-vanishing temperature manifests itself in the flow equations (2.11), (2.14)–(2.16) only through a change to T-dependent threshold functions. In this appendix we will define these functions and discuss some subtleties regarding the definition of the anomalous dimensions and the Yukawa coupling for $T\neq 0$. The corresponding $T=0$ threshold functions can be found in Appendix B where also some of our notation is fixed.

The flow equation (2.11) for the effective average potential involves a bosonic and a fermionic threshold function whose generalization to finite temperature is straightforward:

$$l_n^d(w,\tilde{T};\eta_\Phi) = \frac{(n+\delta_{n,0})}{2}\frac{v_{d-1}}{v_d}k^{2n-d+1}\tilde{T} \times \sum_{l\in\mathbb{Z}}\int_0^\infty dx x^{(d-3)/2} Z_{\Phi,k}^{-1}\frac{\partial_t R_k(y)}{[P(y)+k^2 w]^{n+1}},$$

$$l_n^{(F)d}(w,\tilde{T};\eta_\Phi) = (n+\delta_{n,0})\frac{v_{d-1}}{v_d}k^{2n-d+1} \times \tilde{T}\sum_{l\in\mathbb{Z}}\int_0^\infty dx x^{(d-3)/2} Z_{\psi,k}^{-1} \times \frac{P_F(y_F)}{[1+r_F(y_F)]}\frac{\partial_t[Z_{\psi,k} r_F(y_F)]}{[P_F(y_F)+k^2 w]^{n+1}} \tag{C1}$$

where $\tilde{T}=T/k$ and

$$y = x + (2l\pi T)^2,$$
$$y_F = x + (2l+1)^2\pi^2 T^2. \tag{C2}$$

The computation of the anomalous dimensions η_Φ, η_ψ and the flow equation for the Yukawa coupling h at non-vanishing temperature requires some care. The anomalous dimensions determine the IR cutoff scale dependence of $Z_{\Phi,k}$ and $Z_{\psi,k}$ according to $\eta_\Phi = -\partial_t \ln Z_{\Phi,k}$, $\eta_\psi = -\partial_t \ln Z_{\psi,k}$ with $t=\ln k/k_\Phi$. It is important to realize that for a computation of the scale dependence of the effective three-dimensional $Z_{\Phi,k}$ and $Z_{\psi,k}$ for $T\neq 0$ momentum dependent wave function renormalization constants of the four-dimensional theory are required. This is a consequence of the fact that in the three-dimensional model each of the infinite number of different Matsubara modes of a four-dimensional bosonic or fermionic field $\phi(Q)$ corresponds to a different value of $Q_0 = 2\pi l T$ or $Q_0 = (2l+1)\pi T$, respectively, with $Q^2 = Q_0^2 + \vec{Q}^2$ and $l\in\mathbb{Z}$. We will therefore allow for momentum dependent wave function renormalizations, i.e. for a kinetic part of Γ_k of the form

$$\Gamma_k^{\rm kin} = \int \frac{d^d q}{(2\pi)^d}\{Z_{\Phi,k}(q^2) q^2\ {\rm Tr}(\Phi^\dagger(q)\Phi(q)) + Z_{\psi,k}(q^2)\overline{\psi}(q)\gamma^\mu q_\mu \psi(q)\} \tag{C3}$$

in momentum space.

In the $O(4)$ model the evolution equation for $Z_{\Phi,k}(Q)$ may then be obtained by considering a background field configuration with a small momentum dependence,

$$\Phi_j(x) = \varphi\,\delta_{j1} + (\delta\varphi e^{-iQx} + \delta\varphi^* e^{iQx})\,\delta_{j2}; \quad j=1,\ldots,4 \tag{C4}$$

supplemented by

$$\psi_a = \overline{\psi}_a = 0; \quad a=1,2. \tag{C5}$$

Expanding around this configuration at the minimum of the effective average potential U_k we observe that $\delta\varphi$ corresponds to an excitation in the Goldstone boson direction. The exact inverse two-point function $\Gamma_k^{(2)}$ turns out to be block-diagonal with respect to scalar and fermion indices for this configuration. It therefore decays into corresponding matrices $\Gamma_{Sk}^{(2)}$ and $\Gamma_{Fk}^{(2)}$ acting in the scalar and fermion subspaces, respectively. The scale dependence of the scalar wave function renormalization for non-vanishing T is obtained from Eqs. (1.1) and (C3) for the configuration (C4) as

$$\frac{\partial}{\partial t}Z_{\Phi,k}(Q^2) = \frac{1}{\vec{Q}^2}\left(\lim_{\delta\varphi\,\delta\varphi^*\to 0}\frac{\delta}{\delta(\delta\varphi\,\delta\varphi^*)} \times\left\{\frac{1}{2}{\rm Tr}\left[(\Gamma_{Sk}^{(2)}+R_k)^{-1}\frac{\partial}{\partial t}R_k\right] - {\rm Tr}\left[(\Gamma_{Fk}^{(2)}+R_{Fk})^{-1}\frac{\partial}{\partial t}R_{Fk}\right]\right\} - (\vec{Q}\to 0)\right). \tag{C6}$$

In the three-dimensional theory there is now a different scalar wave function renormalization $Z_{\Phi,k}(Q_0,\vec{Q})$ for each Matsubara mode Q_0. As in the four-dimensional model for $T=0$ we neglect the momentum dependence of the wave function renormalization constants and evaluate $Z_{\Phi,k}$ for $\vec{Q}=0$ for each Matsubara mode. We will furthermore simplify the truncation of the effective average action by choosing the

Matsubara zero-mode wave function renormalization constant for all Matsubara modes, i.e., approximate

$$Z_{\Phi,k}(\tilde{T}) = Z_{\Phi,k}(Q_0^2=0,\vec{Q}^2=0). \tag{C7}$$

This is justified by the rapid decoupling of all massive Matsubara modes within a small range of k for fixed T as discussed in Sec. III. This results in the expression (2.16) for η_Φ but now with temperature dependent threshold functions ($\tilde{T}=T/k$)

$$\begin{aligned}
&m^d_{n_1,n_2}(w_1,w_2,\tilde{T};\eta_\Phi)\\
&\quad = m^d_{n_1,n_2}(w_1,w_2,\tilde{T}) - \eta_\Phi \hat{m}^d_{n_1,n_2}(w_1,w_2,\tilde{T})\\
&\quad = -\frac{1}{2}k^{2(n_1+n_2-1)-d+1}\frac{dv_{d-1}}{(d-1)v_d}\\
&\qquad \times \tilde{T}\sum_{l\in\mathbb{Z}}\int_0^\infty dx x^{(d-1)/2}\frac{\hat{\partial}}{\partial t}\\
&\qquad \times\left\{\frac{\dot{P}(y)}{[P(y)+k^2w_1]^{n_1}}\frac{\dot{P}(y)}{[P(y)+k^2w_2]^{n_2}}\right\}\\
&m^{(F)d}_4(w,\tilde{T};\eta_\psi) = m^{(F)d}_4(w,\tilde{T}) - \eta_\psi \check{m}^{(F)d}_4(w,\tilde{T})\\
&\qquad = -\frac{1}{2}k^{5-d}\frac{dv_{d-1}}{(d-1)v_d}\\
&\qquad\quad \times \tilde{T}\sum_{l\in\mathbb{Z}}\int_0^\infty dx x^{(d-1)/2} y_F\\
&\qquad\quad \times \frac{\hat{\partial}}{\partial t}\left(\frac{\partial}{\partial x}\frac{1+r_F(y_F)}{P_F(y_F)+k^2w}\right)^2.
\end{aligned} \tag{C8}$$

For further technical details we refer the reader to Ref. [27].

The fermion anomalous dimension and the flow equation for the Yukawa coupling can be obtained by considering a field configuration

$$\begin{aligned}
&\Phi_j(x) = \varphi\,\delta_{j1}; \quad j=1,\ldots,4,\\
&\psi_a(x) = \psi_a e^{-iQx},\\
&\overline{\psi}_a(x) = \overline{\psi}_a e^{iQx}; \quad a=1,2.
\end{aligned} \tag{C9}$$

The derivation follows similar lines as for the scalar anomalous dimension discussed above. For computational details we refer the reader to Ref. [27]. An important difference as compared to $Z_{\Phi,k}(Q)$ relates to the fact that there are no fermionic zero modes. It would therefore be inconsistent to define $Z_{\psi,k}(\tilde{T})$ or $h_k(\tilde{T})$ at $Q_0=0$ if Q denotes the external fermion momentum. Yet, we will again resort to the approximation of using the same wave function renormalization constant and Yukawa coupling for all fermionic Matsubara modes. For the same reason as for $Z_{\Phi,k}(\tilde{T})$ we will use for this purpose the mode with the lowest T-dependent mass, i.e. define

$$\begin{aligned}
&Z_{\psi,k}(\tilde{T}) = Z_{\psi,k}(Q_0^2=\pi^2T^2,\vec{Q}^2=0),\\
&h_k(\tilde{T}) = h_k(Q_0^2=\pi^2T^2,\vec{Q}^2=0),
\end{aligned} \tag{C10}$$

where we have neglected a possible dependence of h_k on the external scalar momentum of the Yukawa vertex. This yields the expressions (2.15) and (2.16) for the flow of h^2 and η_ψ, respectively, but now with the T-dependent threshold functions

$$\begin{aligned}
&m^{(FB)d}_{1,2}(w_1,w_2,\tilde{T};\eta_\psi,\eta_\Phi) = m^{(FB)d}_{1,2}(w_1,w_2,\tilde{T}) - \eta_\Phi \hat{m}^{(FB)d}_{1,2}(w_1,w_2,\tilde{T}) - \eta_\psi \check{m}^{(FB)d}_{1,2}(w_1,w_2,\tilde{T})\\
&\qquad = -\frac{1}{2}k^{2(n_1+n_2)-d-1}\frac{dv_{d-1}}{(d-1)v_d}\,\tilde{T}\sum_{l\in\mathbb{Z}}\int_0^\infty dx x^{(d-1)/2}\frac{\hat{\partial}}{\partial t}\left\{\frac{1+r_F(y_F)}{[P_F(y_F)+k^2w_1]^{n_1}}\frac{\dot{P}(y)}{[P(y)+k^2w_2]^{n_2}}\right\},\\
&l^{(FB)d}_{n_1,n_2}(w_1,w_2,\tilde{T};\eta_\psi,\eta_\Phi) = l^{(FB)d}_{n_1,n_2}(w_1,w_2,\tilde{T}) - \eta_\psi \check{l}^{(FB)d}_{n_1,n_2}(w_1,w_2,\tilde{T}) - \eta_\Phi \hat{l}^{(FB)d}_{n_1,n_2}(w_1,w_2,\tilde{T})\\
&\qquad = -\frac{1}{2}k^{2(n_1+n_2)-d+1}\frac{v_{d-1}}{v_d}\,\tilde{T}\sum_{l\in\mathbb{Z}}\int_0^\infty dx x^{(d-3)/2}\frac{\hat{\partial}}{\partial t}\left\{\frac{1}{[P_F(y_F)+k^2w_1]^{n_1}[P(y)+k^2w_2]^{n_2}}\right\}.
\end{aligned} \tag{C11}$$

[1] For a recent review, see H. Meyer-Ortmanns, Rev. Mod. Phys. **68**, 473 (1996).

[2] *Quark Matter '96*, Proceedings of the International Conference on Ultrarelativistic Nucleus-Nucleus Collisions, Heidelberg, Germany, edited by H. Specht *et al.* [Nucl. Phys. **A610**, (1996)].

[3] R. D. Pisarski and F. Wilczek, Phys. Rev. D **29**, 338 (1984).

[4] K. Rajagopal and F. Wilczek, Nucl. Phys. **B399**, 395 (1993); **B404**, 577 (1993).

[5] K. Rajagopal, in *Quark-Gluon Plasma 2*, edited by R. Hwa (World Scientific, Singapore, 1995), hep-ph/9504310.

[6] A. A. Anselm, Phys. Lett. B **217**, 169 (1988); A. A. Anselm and M. G. Ryskin, *ibid.* **266**, 482 (1991); J.-P. Blaizot and A. Krzywicki, Phys. Rev. D **46**, 246 (1992); J. D. Bjorken, Int. J. Mod. Phys. A **7**, 4189 (1992); Acta Phys. Pol. B **23**, 561 (1992); K. L. Kowalski and C. C. Taylor, Report No. CWRUTH-92-6, 1992, hep-ph/9211282; J. D. Bjorken, K. L. Kowalski, and C. C. Taylor, in Proceedings of Les Rencontres de Physique de la Vallée D'Aoste, La Thuile, SLAC-PUB-6109, 1993; in Proceedings of the Workshop on Physics at Current Accelerators and the Supercollider, Argonne, IL, 1993, hep-ph/9309235.

[7] C. M. G. Lattes, Y. Fujimoto, and S. Hasegawa, Phys. Rep. **65**, 151 (1980).

[8] E. Shuryak, Comments Nucl. Part. Phys. **21**, 235 (1994).

[9] C. Wetterich, Nucl. Phys. **B352**, 529 (1991); Z. Phys. C **57**, 451 (1993); **60**, 461 (1993).

[10] C. Wetterich, Phys. Lett. B **301**, 90 (1993).

[11] K. G. Wilson, Phys. Rev. B **4**, 3174 (1971); K. G. Wilson and I. G. Kogut, Phys. Rep., Phys. Lett. **12C**, 75 (1974).

[12] F. Wegner and A. Houghton, Phys. Rev. A **8**, 401 (1973); F. Wegner, in *Phase Transitions and Critical Phenomena*, edited by C. Domb and M. S. Greene (Academic Press, New York, 1976), Vol. 6; J. F. Nicoll and T. S. Chang, Phys. Lett. **62A**, 287 (1977).

[13] S. Weinberg, *Critical Phenomena for Field Theorists* (Erice Subnucl. Phys., 1976), p. 1.

[14] J. Polchinski, Nucl. Phys. **B231**, 269 (1984).

[15] A. Hasenfratz and P. Hasenfratz, Nucl. Phys. **B270**, 685 (1986); P. Hasenfratz and J. Nager, Z. Phys. C **37**, 477 (1988).

[16] C. Wetterich, Z. Phys. C **48**, 693 (1990); S. Bornholdt and C. Wetterich, *ibid.* **58**, 585 (1993).

[17] J. Comellas, Y. Kubyshin, and E. Moreno, Nucl. Phys. **B490**, 653 (1997).

[18] M. Reuter and C. Wetterich, Nucl. Phys. **B391**, 147 (1993); **B408**, 91 (1993); **B417**, 181 (1994); **B427**, 291 (1994); Heidelberg Report No. HD-THEP-94-39.

[19] C. Becchi, Report No. GEF-TH-96-11, hep-th/9607188.

[20] M. Bonini, M. D'Attanasio, and G. Marchesini, Nucl. Phys. **B418**, 81 (1994); **B421**, 429 (1994).

[21] U. Ellwanger, Phys. Lett. B **335**, 364 (1994); U. Ellwanger, M. Hirsch, and A. Weber, Z. Phys. C **69**, 687 (1996).

[22] C. Wetterich, Heidelberg Report No. HD-THEP-95-2, hep-th/9501119; Z. Phys. C **72**, 139 (1996).

[23] U. Ellwanger, M. Hirsch, and A. Weber, Eur. Phys. J. C **1**, 563 (1998).

[24] U. Ellwanger, Z. Phys. C **76**, 721 (1997).

[25] K.-I. Aoki, K. Morikawa, J.-I. Sumi, H. Terao, and M. Tomoyose, Prog. Theor. Phys. **97**, 479 (1997).

[26] U. Ellwanger and C. Wetterich, Nucl. Phys. **B423**, 137 (1994).

[27] D.-U. Jungnickel and C. Wetterich, Phys. Rev. D **53**, 5142 (1996).

[28] D.-U. Jungnickel and C. Wetterich, presented at the Workshop on Quantum Chromodynamics: Confinement, Collisions, and Chaos, Paris, France, 1996, and QCD 96, Yaroslavl, Russia, 1996, hep-ph/9610336.

[29] Y. Nambu and G. Jona-Lasinio, Phys. Rev. **122**, 345 (1961).

[30] J. Bijnens, Phys. Rep. **265**, 369 (1996).

[31] J. Pawlowski, Phys. Rev. D **58**, 045011 (1998).

[32] M. Gell-Mann and M. Levy, Nuovo Cimento **16**, 705 (1960).

[33] M. Gell-Mann, R. J. Oakes, and B. Renner, Phys. Rev. **175**, 2195 (1968).

[34] J. Gasser and H. Leutwyler, Phys. Rep. **87**, 77 (1982); Nucl. Phys. **B250**, 465 (1985).

[35] D.-U. Jungnickel and C. Wetterich, Eur. Phys. J. C **1**, 669 (1998).

[36] D.-U. Jungnickel and C. Wetterich, Phys. Lett. B **389**, 600 (1996).

[37] D.-U. Jungnickel and C. Wetterich, Eur. Phys. J. C **2**, 557 (1998).

[38] J. Adams, J. Berges, S. Bornholdt, F. Freire, N. Tetradis, and C. Wetterich, Mod. Phys. Lett. A **10**, 2367 (1995).

[39] J. Berges and C. Wetterich, Nucl. Phys. **B487**, 675 (1997).

[40] H. Leutwyler, hep-ph/9609467.

[41] M. Jamin and M. Münz, Z. Phys. C **66**, 633 (1995); K. G. Chetyrkin, C. A. Dominguez, D. Pirjol, and K. Schilcher, Phys. Rev. D **51**, 5090 (1995); J. Bijnens, J. Prades, and E. de Rafael, Phys. Lett. B **348**, 226 (1995).

[42] N. Tetradis and C. Wetterich, Nucl. Phys. **B398**, 659 (1993); Int. J. Mod. Phys. A **9**, 4029 (1994).

[43] See for instance J. Kapusta, *Finite Temperature Field Theory* (Cambridge University Press, Cambridge, England, 1989).

[44] P. Ginsparg, Nucl. Phys. **B170**, 388 (1980); T. Appelquist and R. Pisarski, Phys. Rev. D **23**, 2305 (1981); S. Nadkarni, *ibid.* **27**, 917 (1983); N. P. Landsman, Nucl. Phys. **B322**, 498 (1989).

[45] N. Tetradis and C. Wetterich, Nucl. Phys. **B422 [FS]**, 541 (1994).

[46] B. Widom, J. Chem. Phys. **43** 3898 (1965).

[47] J. Berges, N. Tetradis, and C. Wetterich, Phys. Rev. Lett. **77**, 873 (1996).

[48] D. Toussaint, Phys. Rev. D **55**, 362 (1997).

[49] E. Brezin, D. J. Wallace, and K. G. Wilson, Phys. Rev. B **7**, 232 (1973).

[50] K. Kanaya and S. Kaya, Phys. Rev. D **51**, 2404 (1995).

[51] G. Baker, D. Meiron, and B. Nickel, Phys. Rev. B **17**, 1365 (1978).

[52] J. Zinn-Justin, *Quantum Field Theory and Critical Phenomena* (Oxford University Press, New York, 1993).

[53] T. R. Morris and M. D. Turner, Nucl. Phys. **B509**, 637 (1998).

[54] P. Butera and M. Comi, Phys. Rev. B **52**, 6185 (1995).

[55] T. Reisz, Phys. Lett. B **360**, 77 (1995).

[56] C. Bernard *et al.*, Phys. Rev. D **55**, 6861 (1997); C. Bernard *et al.*, Nucl. Phys. B (Proc. Suppl.) **53**, 442 (1997).

[57] S. Gottlieb *et al.*, Phys. Rev. D **55**, 6852 (1997).

[58] F. Karsch, Phys. Rev. D **49**, 3791 (1994); F. Karsch and E. Laermann, *ibid.* **50**, 6954 (1994).

[59] Y. Iwasaki, K. Kanaya, S. Kaya, and T. Yoshie, Phys. Rev. Lett. **78**, 179 (1997).

[60] G. Boyd, F. Karsch, E. Laermann, and M. Oevers, talk given at 10th International Conference on Problems of Quantum Field Theory, Alushta, Ukraine, 1996, hep-lat/9607046.

[61] A. Ukawa, Nucl. Phys. B (Proc. Suppl.) **53**, 106 (1997); S. Aoki, T. Kaneda, A. Ukawa, and T. Umemura, *ibid.* **53**, 438 (1997).

[62] J. Gasser and H. Leutwyler, Phys. Lett. B **184**, 83 (1987); H. Leutwyler, Nucl. Phys. B (Proc. Suppl.) **4**, 248 (1988).

[63] C. Bernard *et al.*, Phys. Rev. Lett. **78**, 598 (1997).

[64] J. B. Kogut, J. F. Lagae, and D. K. Sinclair, Nucl. Phys. B (Proc. Suppl.) **53**, 269 (1997).